

Origin of serpentinite-related nephrite from Jordanów and adjacent areas (SW Poland) and its comparison with selected nephrite occurrences

Grzegorz GIL^{1,*}, Jaime D. BARNES², Chiara BOSCHI³, Piotr GUNIA¹, György SZAKMÁNY⁴, Zsolt BEND⁴, Paweł RACZY SKI¹ and Bálint PÉTERDI⁵

- 1 University of Wrocław, Institute of Geological Sciences, Pl. Maksa Borna 9, 50-205 Wrocław, Poland
- 2 Jackson School of Geosciences, University of Texas at Austin, Department of Geological Sciences, 2275 Speedway Stop C9000, Austin, Texas 78712, USA
- 3 The National Research Council, Institute for Geosciences and Earth Resources, Via Moruzzi 1, 56124 Pisa, Italy
- 4 Eötvös Loránd University, Institute of Geography and Earth Sciences, Pazmany Peter Setany 1/C, H-1117 Budapest, Hungary
- 5 Geological and Geophysical Institute of Hungary, Department of Geological and Geophysical Collections, Stefánia út 14, H-1143 Budapest, Hungary



Gil, G., Barnes, J.D., Boschi, C., Gunia, P., Szakmány, G., Bend, Z., Raczki, P., Péterdi, B., 2015. Origin of serpentinite-related nephrite from Jordanów and adjacent areas (SW Poland) and its comparison with selected nephrite occurrences. *Geological Quarterly*, 59 (3): 457–472, doi: 10.7306/gq.1228

The Gogołów-Jordanów Massif (GJM) in the Fore-Sudetic Block, SW Poland, hosts nephrites traditionally interpreted as serpentinite-related (ortho-nephrite). This contribution confirms the serpentinite-related origin of the nephrites on the basis of mineralogy, bulk-rock chemistry, and O and H isotopes. Rock-forming amphiboles from nephrites of the GJM have 7.73–7.99 Si apfu, comparable to 7.76–8.03 Si apfu of serpentinite-related Crooks Mountain nephrite amphibole (Granite Mountains, Wyoming, USA). The GJM amphiboles also have Mg/(Mg + Fe²⁺) values ranging from 0.82 to 0.94, similar to serpentinite-related Crooks Mountain and New Zealand nephrites amphiboles with Mg/(Mg + Fe²⁺) values of 0.86–0.90 and 0.91 to 0.92, respectively. The GJM nephrite amphiboles differ from the Val Malenco dolomite-related nephrite (Italy) amphibole, e.g., Val Malenco has a higher Si content (~8.0 Si apfu), although it overlaps with some of the GJM nephrite samples, and ~1.0 Mg/(Mg + Fe²⁺), also higher than the GJM samples. Also, apatite in the nephrite studied from the GJM has a slightly higher Ca content than apatite from dolomite-related nephrite. Chlorites found in the Jordanów nephrite have similar compositions to that of chlorites in the serpentinite-related nephrites and also to chlorites associated with serpentinisation/rodingitisation. The bulk-rock FeO vs. Fe/(Fe + Mg), Cr, Ni, and Co are also typical of the serpentinite-related nephrites. The δ¹⁸O values range from +6.1 to +6.7‰ (±0.1‰), and the average δD values = –61‰, corresponding with the serpentinite-related nephrites range. Based on petrographic observations, we suggest four crystallisation stages (including rodingitisation prior to nephrite formation): 1 – leucogranite rodingitisation and black-wall formation; 2 – tremolite formation at the expense of rodingite diopside and black-wall chlorite (nephritisation) and garnet break-down, with spinel and chlorite formation (chlorite can be a product of garnet break-down or spinel with serpentine reaction); 3 – prehnite vein formation; 4 – tremolite formation at the expense of prehnite veins and actinolite veins formation. Spinels composed of 0.29–1.96 wt.% MgO, 24.87–29.67 wt.% FeO, 8.72–22.82 wt.% Fe₂O₃, 3.11–4.36 wt.% Al₂O₃, and 39.07–54.46 wt.% Cr₂O₃ suggest nephritisation in the greenschist to lower-amphibolite-facies conditions.

Key words: nephrite, serpentinite-related nephrite, ortho-nephrite, stable isotopes, Gogołów-Jordanów Massif, Jordanów (Jordansmühl), Naslawice (Naselwitz, Steinberge).

INTRODUCTION

Nephrite (nephrite jade) is one of the two forms of jade, the other being jadeite. Nephrite is a monomineral amphibole rock, composed of fibrous tremolite and/or actinolite, forming

an interlocking fabric, also known as nephritic texture. This interlocking fibrous fabric results in an extreme toughness, combined with a relatively low hardness (ca. 5.5–6.5 in Mohs' scale), making nephrite a valuable carving material. Nephrite has been used since the Early Neolithic period and currently is primarily used for the carving of decorative items and jewellery.

The largest nephrite deposits are located in British Columbia (Canada; Simandl et al., 2000; Makepeace and Simandl, 2001), Wyoming, California, and Alaska (USA; Sinkankas, 1959; Sherer, 1972; Middleton, 2006), Siberia (Russia; Harlow and Sorensen, 2001, 2005; Łapot, 2004; Kostov et al., 2012), Xinjiang, Qinghai, Liaoning, Jiangsu, Sichuan and Henan

* Corresponding author, e-mail: grzegorz.gil@ing.uni.wroc.pl; grzegorz.gil@mailplus.pl

Received: November 24, 2014; accepted: February 12, 2015; first published online: April 13, 2015

(China; Liu et al., 2010, 2011a, b; Siqin et al., 2012), Chuncheon (Korea; Yui and Kwon, 2002), Hualien (Taiwan; Wan and Yeh, 1984; Siqin et al., 2012), South Australia and New South Wales (Australia; Aitchison et al., 1992; Harlow and Sorensen, 2001, 2005), and the South Island (New Zealand; Middleton, 2006; Adams et al., 2007; Grapes and Yun, 2010). There are also nephrite deposits in Europe – Sondrio (Italy; Adamo and Bocchio, 2013), Scortaseo (Switzerland; Dietrich and de Quervain, 1968; Adamo and Bocchio, 2013; Péterdi et al., 2014), Thuringia and Bavaria (Germany; Łobos et al., 2008; Péterdi et al., 2014), and Usinmaki and Pakila (Finland; Gunia, 2000). In addition, there are at least two nephrite-bearing areas in Lower Silesia (SW Poland) – the Gogołów-Jordanów Massif (GJM) and Złoty Stok (former German name Reichenstein; Traube, 1885a, b, 1887, 1888; Sachs, 1902; Beutell and Heinze, 1914; Maciejewski, 1966; Heflik, 1974, 2010; Majerowicz, 2006; Middleton, 2006; Gil, 2011, 2013). Within the GJM, two major occurrences are distinguished – Jordanów (German name Jordansmühl) and Nasławice (German names Naselwitz and Steinberge; Majerowicz, 2006; Łobos et al., 2008; Gil, 2013). The Lower Silesian deposits place Poland amongst the largest nephrite-bearing areas in Europe (Heflik, 1974; Middleton, 2006; Łobos et al., 2008; Gil, 2013). These deposits are also amongst the earliest-discovered, in the 1880s (Traube, 1885a, b, 1887, 1888; Sachs, 1902; Beutell and Heinze, 1914; Maciejewski, 1966; Middleton, 2006; Heflik, 2010).

Nephrite can be divided into serpentinite-related (ortho-nephrite) and dolomite-related (para-nephrite), depending on origin (Harlow and Sorensen, 2005; Middleton, 2006). Serpentinite-related nephrite forms at the contact between serpentinite or peridotite with more silicic rocks (usually a granitic intrusion, rodingitised plagiogranite, or metasediment). Dolomite-related nephrite forms at the contact between dolomitic marble and a granitic intrusion (cf. Harlow and Sorensen, 2001, 2005; Yui and Kwon, 2002). The proposed metasomatism during serpentinite-related nephrite formation assumes SiO₂ migration from rodingitised rock through the black-wall and Ca migration from rodingitised rock and/or from serpentinitising peridotite through

black-wall (Harlow and Sorensen, 2005 and references therein). Clinopyroxene breakdown is a likely Ca source for nephritisation. Apart from the geological position and petrographic association, the serpentinite-related nephrites differ from dolomite-related ones in minor mineral constituents and accessory phases, mineral chemistry, bulk-rock trace elements, and O and H isotope ratios. The elemental concentrations of Cr, Ni, and Co and the Fe/Mg ratio in rock-forming minerals and bulk-rock composition are diagnostic of its origin (Harlow and Sorensen, 2005; Middleton, 2006; Liu et al., 2011a, b). However, these concentrations can overlap (as shown in Table 1), so conclusions about serpentinite-related or dolomite-related origin should be based on multiple observations. For example, rock-forming amphiboles of serpentinite-related nephrites usually have higher Cr₂O₃ (0.02–0.43 wt.%; see Table 1; Grapes and Yun, 2010; Liu et al., 2011a) than dolomite-related nephrites (0.00–0.09 wt.%; Liu et al., 2011a; Ling et al., 2013), although several studies (Liu et al., 2010, 2011b) described dolomite-related nephrite amphiboles with elevated Cr₂O₃ (0.03–1.18 wt.%). Amphiboles NiO and diopside Cr₂O₃ are also characteristic (both higher in serpentinite-related nephrite; Table 1), but unfortunately, NiO is usually not included in standard nephrite amphiboles electron microprobe analyses. Serpentinite-related nephrites tend to have bulk-rock Cr concentrations between 900 and 2812 ppm, Ni between 959 and 1898 ppm, and Co between 42 and 207 ppm, whereas dolomite-related varieties have lower Cr concentrations, between 2 and 179 ppm, Ni between 0.05 and 471 ppm, and Co between 0.5 and 10 ppm (Table 1; Grapes and Yun, 2010; Liu et al., 2011b; Kostov et al., 2012; Siqin et al., 2012). Siqin et al. (2012) shows that serpentinite-related nephrites have bulk-rock Fe/(Fe + Mg) >0.060, whereas most dolomite-related nephrites are <0.060, although there is some overlap and some dolomite-related nephrites also have a Fe/(Fe + Mg) ratio >0.060. Serpentinite-related nephrites tend to have δ¹⁸O values between 4.5 and 9.6‰, and δD values between –67 and –33‰ (Yui et al., 1988; Yui and Kwon, 2002), whereas dolomite-related nephrites have δ¹⁸O values between –9.9 and 6.2‰, and δD

Table 1

Selected characteristic features of the serpentinite-related and dolomite-related nephrites compiled from published data and our analyses

Sample	Feature	Serpentinite-related nephrite	Dolomite-related nephrite
Amphibole	Cr ₂ O ₃ wt.%	0.08–0.36 ^c ; 0.07–0.43 ^e ; 0.020–0.127 ^k	0.39–1.14 ^d ; 0.00–0.07 ^a ; 0.03–1.18 ^f ; <0.05–0.09 ^j
	NiO wt.%	0.08–0.25 ^c ; 0.08–0.36 ^e	0.00–0.08 ^e ; <0.05–0.06 ^j
	δ ¹⁸ O‰	4.5–5.3 ^a ; 6.9–9.6 ^b	–9.9 to –8.2 ^b ; 0.5–3.4 ^b ; 1.1–5.6 ^e ; 3.2–6.2 ^f
	δD‰	–67 to –33 ^a ; –54 to –39 ^b	–114 to –105 ^b ; –124 to –56 ^b ; –72.4 to –55.7 ^e ; –94.7 to –83.0 ^f ; –113 ± 4.8 ^j
Diopside	Cr ₂ O ₃ wt.%	0.018–0.640 ^k	0.00–0.03 ^f
Bulk-rock	Cr ppm	1220–1890 ^c ; 900–1113 ^g ; 1505.3–2812.1 ^h	8.95–178.70 ^f ; 1.9–67.9 ^h
	Ni ppm	1199–1484 ^c ; 1887–1898 ^g ; 958.7–1304.4 ^h	0.05–3.95 ^f ; 22.2–470.7 ^h
	Co ppm	204–207 ^g ; 42.0–53.0 ^h	0.5–9.8 ^h
	Fe/(Fe + Mg)	above 0.060 ^h	usually below 0.060 ^h

a – Yui et al. (1988); b – Yui and Kwon (2002); note: b – detailed study of dolomite-related Chuncheon nephrite (many analyses), b' – compilation of single analyses from several serpentinite-related and dolomite-related nephrite deposits (other than Chuncheon), both from the same work, for details see also Figure 11; c – Grapes and Yun (2010); d – Liu et al. (2010); e – Liu et al. (2011a); f – Liu et al. (2011b); g – Kostov et al. (2012), data without Jordanów nephrite, discussed extensively in present paper; h – Siqin et al. (2012), Cr, Ni and Co recalculated from wt.%; i – Adamo and Bocchio (2013); j – Ling et al. (2013); k – present study of comparable material from Crooks Mountain and New Zealand nephrites, for details see Appendix 2

values between -124 and -56‰ (Yui and Kwon, 2002; Liu et al., 2011a, b; Adamo and Bocchio, 2013).

Nephrites in the GJM were interpreted as serpentinite-related (ortho-nephrite), due to their occurrence within a serpentinite massif (Maciejewski, 1966; Gunia, 2000; Harlow and Sorensen, 2005; Middleton, 2006; Łobos et al., 2008). However, detailed mineralogical and geochemical studies which would support this interpretation are missing. The present paper provides an overview of recent studies on the GJM nephrites, presents new mineralogical and geochemical data that focus on their origin, and discusses geochemical data compared with nephrites worldwide. The GJM nephrites light isotope compositions have never been analysed before. Until now, there were only $\delta^{18}\text{O}$ and δD of serpentines from Jordanów and Nasławice (J drysek et al., 1991), and $\delta^{18}\text{O}$ and $\delta^{13}\text{C}$ of magnesite from Nasławice (J drysek and Hałas, 1990), therefore our nephrite O and H isotope study provides original new data. We also present new results on the GJM nephrite mineral chemistry and new petrographic and microprobe results on serpentinite-related nephrites from Crooks Mountain (the Granite Mountains, Wyoming, USA) and the South Island (New Zealand). Finally, we propose the crystallisation sequence of the GJM nephrites.

GEOLOGICAL SETTING

Jordanów (or Jordanów I ski in full) and Nasławice are located in Lower Silesia (SW Poland), ca. 25 km SSW of Wrocław. Nasławice lies 3 km NW from Jordanów. The two nephrite-bearing quarries, Jordanów and Nasławice, are ca. 2 km from one another. Both quarries are situated in serpentinites of the GJM, and are covered by Cenozoic deposits. The area studied is located in the strongly peneplained Fore-Sudetic Block, separated by the Sudetic Boundary Fault from the Sudetes Mountains in the west and south. The entire area forms the NE edge of the Bohemian Massif. The Sudetes (together with the Fore-Sudetic Block) are divided into the West, Central, and East Sudetes, composed of tectono-stratigraphic units juxtaposed during the Variscan orogeny (Mazur et al., 2006). The area studied lies in the Central Sudetes sector (Fig. 1), which is composed of the Góry Sowie, Orlica, nie nik, Kłodzko, and Kamieniec medium- to high-grade, Neoprotero-

zoic-Lower Paleozoic metamorphic units, and the Ordovician-Lower Carboniferous Bardo Sedimentary Unit, Lower Devonian Central Sudetic Ophiolite, Niemcza and Skrzyńka Shear zones, and several smaller units, and a number of Variscan granitic plutons, in which the Strzegom-Sobótka is one of the largest (Fig. 2A; Mazur et al., 2006).

The GJM is the lowermost part (built of serpentinites; geographically southern and eastern) of the I a Ophiolite, which belongs to the Central Sudetic Ophiolite – a dismembered unit bordering the Góry Sowie Massif from the N, E, S, and SW (Majerowicz, 1963, 1979, 1984, 2006; Jamrozik, 1981a, b; Narbski et al., 1982; Borkowska et al., 1989; Gunia, 1992; Mierzejewski and Abdel-Wahed, 2000; Mazur et al., 2006; Kryza and Pin, 2010; Kryza, 2011). Central Sudetic Ophiolite consists of the four major ophiolites: the Nowa Ruda Massif in the south, comprising peridotites and serpentinites, gabbros, diabases, and pillow lavas, metamorphosed in low grade, up to greenschist facies; the Braszowice Massif in the south-east, comprising serpentinites and deformed gabbros, containing rodingites; the Szklary Massif in the east, comprising weathered serpentinites, also containing rodingites; the I a Ophiolite in the north, comprising serpentinitised peridotites, ultramafic cumulates (rich in pyroxene and amphibole), metagabbros, diabases (sheeted dykes), metabasalts (pillow lavas), plagiogranite and rodingite bodies, and dark radiolaria-bearing metacherts (Majerowicz, 1984; Dubińska, 1995; Kryza and Pin, 2010; Heflik et al., 2014 and references therein). The N–S trending Niemcza Shear Zone separates the Góry Sowie Massif from the Kamieniec Metamorphic Belt, and is interpreted as mylonitised Góry Sowie gneisses (Mazur et al., 2006). The Niemcza Shear Zone is composed of mylonites, with subordinate non-mylonitised gneiss and mica-schist lenses, Variscan granitoid dykes, and also hosts parts of the Central Sudetic Ophiolite – e.g., the Szklary and Braszowice ophiolites.

The nephrites studied occur within serpentinites of the I a Ophiolite (Fig. 2B). These serpentinites are adjacent to the Niemcza Shear Zone (to the south), Paleozoic metasedimentary rocks (mostly phyllite and black meta-siliceous shales, and minor granitogneiss; to the east), the upper segments of the I a Ophiolite (metagabbros and amphibolites; to the west and north-west), and to the Variscan Strzegom-Sobótka Granite, several kilometres farther W and NW (Fig. 2B; Gaździk, 1960; Trepka and Mierzejewski, 1961; Mierzejewski and Abdel-Wahed, 2000; Kryza, 2011). The I a Ophiolite is the largest and best-studied part of the Central Sudetic Ophiolite, is relatively well-preserved, and shows MOR characteristics (Kryza and Pin, 2010). Serpentinites build southern and eastern ophiolite parts (ca. 100 km²), metagabbros build central parts, and metadiabases and metabasalts build northern parts (Gaździk, 1960; Trepka and Mierzejewski, 1961; Mierzejewski and Abdel-Wahed, 2000). GJM serpentinites comprise pseudomorphic lizardite-chrysotile type serpentinite blocks (early low-temperature, zeolite facies metamorphism), adjoining the massive, non-pseudomorphic antigorite type serpentinites (greenschist facies metamorphism), and also contain serpentinite mylonites rich in chrysotile. Serpentinites adjacent to black-walls are generally antigorite rich (cf. Majerowicz, 1984; Dubińska et al., 2004). Ultrabasites represent serpentinitised harzburgites and Iherzolites equilibrated in the spinel-peridotite stability field, although the spinel-pyroxene domains observed are interpreted as garnet breakdown products (Dubińska et al., 2004). The contact of serpentinites with gabbros is strongly tectonised, and the entire ophiolite is in intrusive contact with the Strzegom-Sobótka Granite (Kryza and Pin, 2010). Two varieties of rodingites were documented in the GJM: boninitic rodingite and plagiogranitic rodingite. These rocks experienced several episodes of brittle

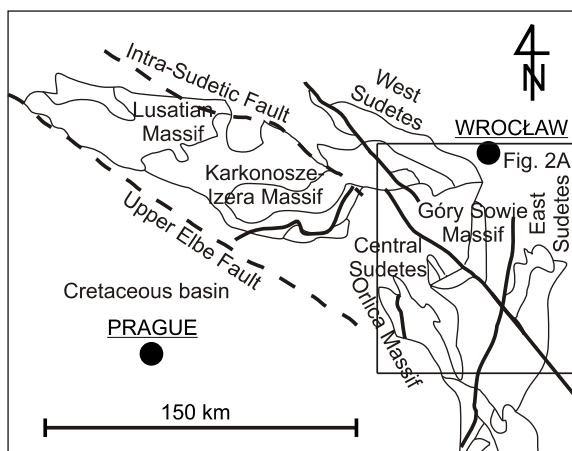


Fig. 1. Schematic geological map of the NE Bohemian Massif (modified after Matte et al., 1990, fide Mazur et al., 2006), with indicated East, Central and West Sudetes

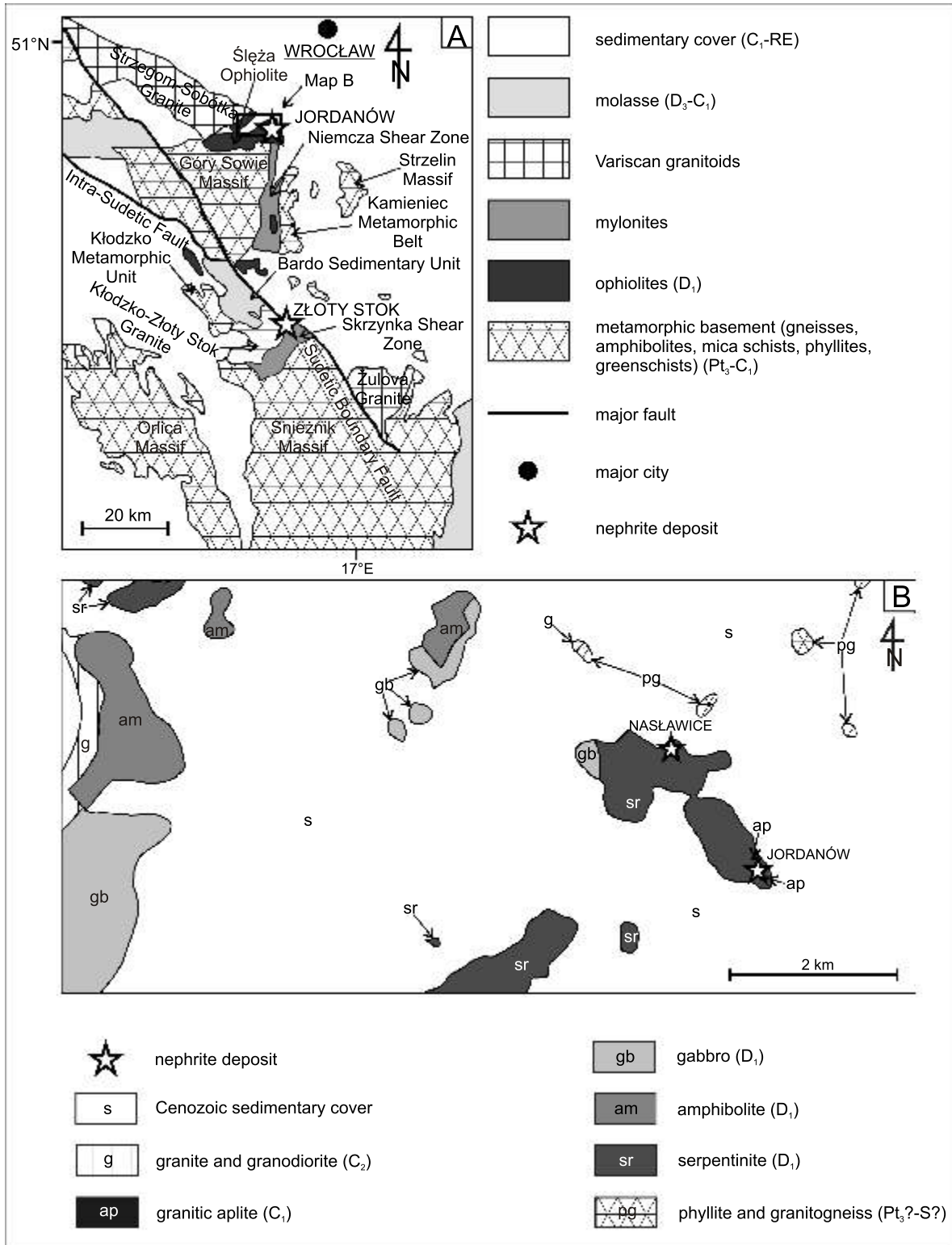


Fig. 2A – simplified geological map of the Sudetes (legend on the right), modified after Aleksandrowski et al. (1997, fide Mazur et al., 2006); B – detailed geological map of the eastern part of the I a Ophiolite – nephrite-bearing eastern part of the Gogołów-Jordanów Massif (legend below), modified after Gaździk (1960) and Trepka and Mierzejewski (1961)

deformation (Dubiska, 1995; Dubiska et al., 2004 and references therein). Rodingites are composed of grossular, hydrogrossular, diopside, augite, chlorite, and vesuvianite, and contain relict and accessory phases: clinozoisite, zoisite, prehnite, tremolite, talc, albite, anorthite, K-feldspar, titanite, apatite,

magnesite, spinel, sphalerite, and galena (Majerowicz, 1979, 1984; Dubiska, 1995; Dubiska et al., 2004; Heflik et al., 2014). The black-wall thickness varies from a few centimetres to ca. 1 m. The black-walls surrounding rodingite dykes are heterogeneous and composed of two clast types: coarse-crystalline com-

posed of chlorite with minor ilmenite, and homogeneous clayey clasts containing corrensite. In general, black-walls are composed of clinocllore and corrensite, and contain minor ilmenite, apatite, zircon, magnetite, hematite, opal and chalcedony (Dubińska et al., 2004). In some works, the black-wall is divided into mineral zones, i.e. the quartz-zoisite zone adjacent to rodingite/plagiogranite, the quartz-zoisite-tremolite zone, the talc schist, and the talc-chlorite schist adjacent to serpentinite (cf., Gunia, 2000; Péterdi et al., 2014). These zones can reflect the intensity of metasomatic influx.

Nephrite in the area studied occurs within chlorite black-walls, at the contact between rodingitised dykes and host-serpentinites (Fig. 3A, B). The rodingitised dyke orientation varies from vertical to horizontal. In addition, single rodingitised dykes with changing orientations are observed. The black-wall thickness varies from several centimetres to ~1 m. Nephrite occurs as irregular veins and nests with variable directions and strike, within the black-walls, which are < ~50 cm thick. Historically, nephrite bodies up to ~1.5 m long and ~0.5 m thick and weighing > ~2 tons were excavated (cf., Gil, 2013). In addition to completely rodingitised dykes, partially-rodingitised leucogranite veins are also present. The serpentinitisation and rodingite black-wall formation age, based on the U-Pb age of zircon from a black-wall, was assumed to be 400 ± 4 – 3 Ma (Dubińska et al., 2004); however, a similar age (400 ± 10 Ma), obtained by SHRIMP U-Pb method on zircon from gabbros, was assumed as the magmatic ophiolite age (Kryza and Pin, 2010). The U-Pb zircon age of a leucogranite vein from Jordanów is 337 ± 4 Ma (Kryza, 2011). This leucogranite age corresponds with granitoid veins from the Niemcza Shear Zone (338 ± 2 – 3 Ma; Oliver et al., 1993), rather than with the Strzegom-Sobótka Granite (~310–294 Ma; cf., Kryza, 2011). Recent work determines the Strzegom-Sobótka Granite to be between 304.8 ± 2.7 Ma and 294.4 ± 2.7 Ma (Turniak et al., 2014), younger than the leucogranite from Jordanów.

MATERIALS AND METHODS

Field studies were performed in the historical, abandoned quarry at Jordanów, and in the active quarry at Nasławice. In the Jordanów Quarry, samples were collected directly from the quarry walls, mostly from a black-wall at the contact of partially-rodingitised leucogranite. In contrast, no nephrite samples were found at Nasławice. It is assumed that earlier-reported nephrite from that quarry was either exploited or all accessible nephrite has been removed by mineral collectors. Therefore, the Nasławice nephrite description and mineral chemistry presented here are from Łobos et al. (2008). For comparison, Crooks Mountain (Granite Mountains, Wyoming, USA) and South Island (New Zealand) serpentinite-related nephrites were obtained for investigation from the University of Wrocław Mineralogical Museum collection.

The field-collected and museum samples were thin-sectioned and examined under a *Nikon Eclipse E600 POL* standard petrographic microscope, whereas cathodoluminescence (CL) petrology was performed on thin sections under the cold cathodoluminescence instrument Cambridge Image Technology Ltd. CL mk3a, equipped with a *Nikon Eclipse E400 POL* petrographic microscope (both at the Institute of Geological Sciences, the University of Wrocław). CL observations were performed under 12.0–14.0 kV voltage, and 400–500 mA current. Several of the field-collected samples were investigated under the *AMRAY 1830* scanning electron microscope (SEM) with an energy-dispersive spectrometer (EDS) at the Institute of Geography and Earth Sciences (Eötvös Loránd University, Budapest, Hungary), under 20.0 kV acceleration voltage, 1.0 nA beam current, and 50–100 nm beam diameter. Mineral chemical composition was determined using a *Cameca SX 100* electron microprobe (EMPA) with EDS and wavelength-dispersive spectrometers (WDS), in the Microscopy and Microprobe Laboratory (Warsaw University, Poland). Analyses were performed

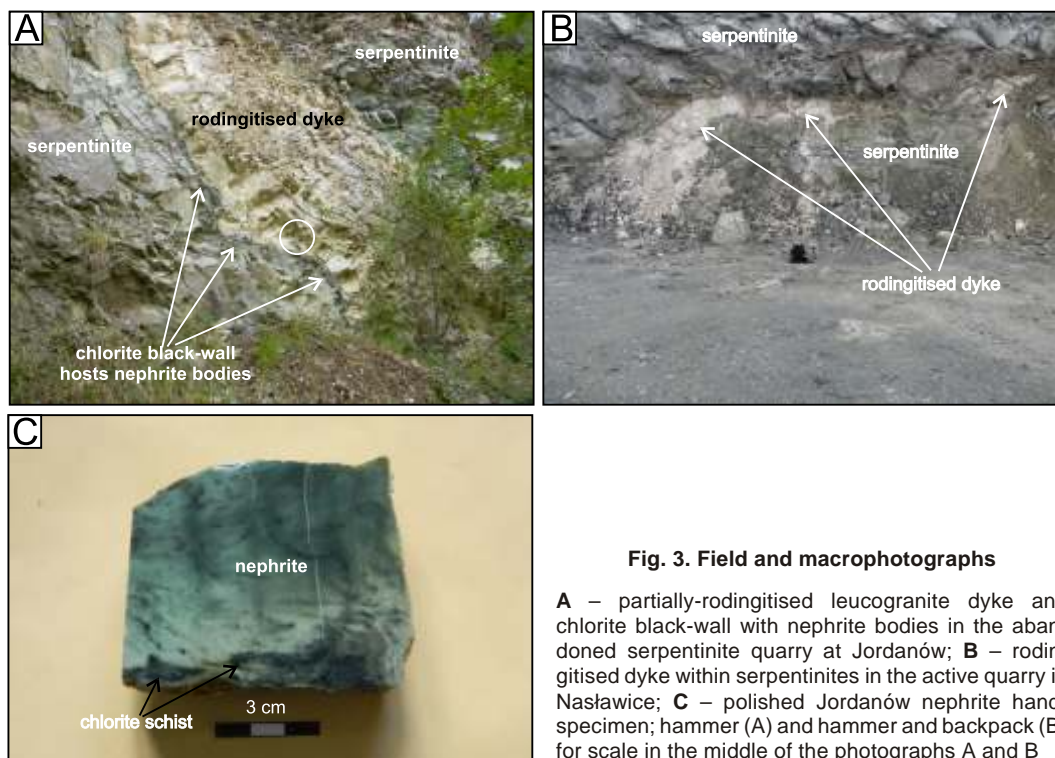


Fig. 3. Field and macrophotographs

A – partially-rodingitised leucogranite dyke and chlorite black-wall with nephrite bodies in the abandoned serpentinite quarry at Jordanów; **B** – rodingitised dyke within serpentinites in the active quarry in Nasławice; **C** – polished Jordanów nephrite hand-specimen; hammer (A) and hammer and backpack (B) for scale in the middle of the photographs A and B

with a 15.0 kV acceleration voltage and 10.0 and 20.0 nA beam current. The FeO and Fe₂O₃ ratios in spinels and garnets were calculated by charge balance, assuming ideal stoichiometry, using the *Cameca SX 100* routine. The analyses were recalculated from oxides in weight percent (wt.%) to atoms per formula unit following the method of [Leake et al. \(1997\)](#).

The Jordanów nephrite bulk-rock chemical composition was determined by prompt-gamma neutron activation analysis (PGAA) by [Péterdi et al. \(2014\)](#) in the PGAA Laboratory of the Budapest Neutron Centre (Hungary). However, [Péterdi et al. \(2014\)](#) did not mention all measured oxides/elements, hence the composition cited is complemented by some previously unpublished elemental concentrations (cf. [Table 2](#)). In [Table 2](#) we also present major oxide and trace element concentrations of Jordanów nephrite, performed by means of the proton microbeam particle-induced X-Ray emission (micro-PIXE), by [Kostov et al. \(2012\)](#).

Table 2

Jordanów nephrite bulk-rock chemical composition measured by the prompt-gamma neutron activation analysis (PGAA), and proton microbeam particle-induced X-Ray emission (micro-PIXE); Fe₂O₃ recalculated from FeO

[wt.%]	PGAA	micro-PIXE
SiO ₂	56.70 ^a	56.63 ^b
TiO ₂	0.0048	<0.0025 ^b
Al ₂ O ₃	2.33 ^a	0.98 ^b
Fe ₂ O _{3(tot)}	3.89 ^a	4.61 ^b
MnO	0.127 ^a	0.029 ^b
MgO	21.30 ^a	22.82 ^b
CaO	12.40 ^a	13.39 ^b
Na ₂ O	0.05 ^a	0.03 ^b
K ₂ O	<0.02	0.00 ^b
H ₂ O	2.84 ^a	
SO ₃	<0.05	<0.01 ^b
As ₂ O ₃	<0.50	
Total	99.642	98.489
[ppm]		
P		178 ^b
B	1.6	
Cl	<10	<35 ^b
V	<40	86 ^b
Cr	1220	719 ^b
Co	47	260 ^b
Ni	1408	1623 ^b
Cu		4 ^b
Zn		84 ^b
Nd	<5	
Sm	<0.5	
Gd	<0.5	
FeO [ppm]	35003	41500
Fe/(Fe + Mg)	0.084	0.093

a – after [Péterdi et al. \(2014\)](#); b – after [Kostov et al. \(2012\)](#); 0.00 – concentration below detection limit; <0.02 – below given detection limit; (empty space) – not analysed

The oxygen isotope composition of two nephrite samples was determined using the laser fluorination method of [Sharp \(1990\)](#). Samples were crushed and ~2.0 mg nephrite fragments were picked under a binocular microscope to ensure a homogeneous sample (i.e., no inclusions). The samples were heated with a *New Wave Research MIR10-30* laser in the presence of BrF₅, and the purified O₂ was then introduced into a *Thermo-Electron MAT 253* mass spectrometer, housed in the Department of Geological Sciences (Jackson School of Geosciences, University of Texas at Austin, USA). In order to check for the precision and accuracy of the analyses, garnet standard UWG-2 ($\delta^{18}\text{O}$ value = +5.8‰) ([Valley et al., 1995](#)) and quartz standard Lausanne-1 ($\delta^{18}\text{O}$ value = +18.1‰) were run. All $\delta^{18}\text{O}$ values are reported relative to SMOW, where the $\delta^{18}\text{O}$ value of NBS-28 (biotite) is +9.65‰. The precision is $\pm 0.1\text{‰}$. The hydrogen isotope composition of powdered nephrite samples was measured using the *Finnigan MAT Delta Plus* isotope ratio mass spectrometer, coupled with a thermal conversion elemental analyser (TC/EA-IRMS) in the Institute for Geosciences and Earth Resources of The National Research Council of Italy in Pisa (CNR-IGG). The measured isotopic composition is expressed in per mil notation relative to Standard Mean Ocean Water (SMOW) and normalised to a biotite NBS-30 standard (D value = -65‰). The precision is $\pm 2\text{‰}$.

PETROLOGY, MINERALOGY, BULK-ROCK GEOCHEMISTRY, AND ISOTOPIC CHARACTERISTICS OF NEPHRITE

PETROGRAPHY

The Jordanów nephrite's ([Fig. 3C](#)) general appearance is typical of most nephrites, i.e., chaotic, flat-parallel or wavy fabric, and transparency from semitranslucent to opaque. The presence of chlorite schist, serpentinite and rodingite nests, and layers in some of the nephrite samples is visible macroscopically. Black spinels in nephrite locally form a spotted texture. Nephrite is white, greenish-creamy, bluish-green, and most commonly bright to dark green; the rock luster is usually waxy or greasy ([Traube, 1885a, b, 1888](#); [Sachs, 1902](#); [Heflik, 1974](#); [Gunia, 2000](#); [Gil, 2013](#)). Under the petrographic microscope ([Fig. 4A](#)), nephrite shows typical chaotic fabric (close intergrowths of fine tremolite fibers) and minor foliated zones (flat-parallel or folded). The tremolite fibers' size is usually ca. 10–60 μm , whereas tremolite porphyroblasts can reach up to ~0.6 mm (600 μm). Samples can be divided into nephrite *sensu stricto* and nephrite schist (cf., [Gil, 2013](#)). Nephrite is composed of tremolite (87.2–89.8 vol.%), diopside (4.7–5.7 vol.%), chlorite (3.8–8.1 vol.%), Cr-spinel (trace, to 0.2 vol.%), and grossular garnet (absent, to 0.5 vol.%); whereas, the nephrite schist (resembling semi-nephrite, also hydrothermally altered semi-nephrite) is composed of tremolite (33.5–79.7 vol.%, although in transition to rodingite and chlorite schist, the tremolite content can drop to 11.4 vol.%), diopside (7.4–55.1 vol.%), chlorite (5.0–38.9 vol.%), Cr-spinel (trace, to 4.2 vol.%), grossular garnet (trace, to 10.8 vol.%), prehnite (absent, to 0.5 vol.%), titanite (trace, to 0.8 vol.%), and opaque + clay minerals-oxides aggregates (trace, to 9.7 vol.%; [Gil, 2013](#)). Hydrothermally-altered semi-nephrite samples are especially rich in opaque + clay minerals-oxide aggregates. The transition from nephrite to nephrite schist is common on a single specimen-scale. The other accessory

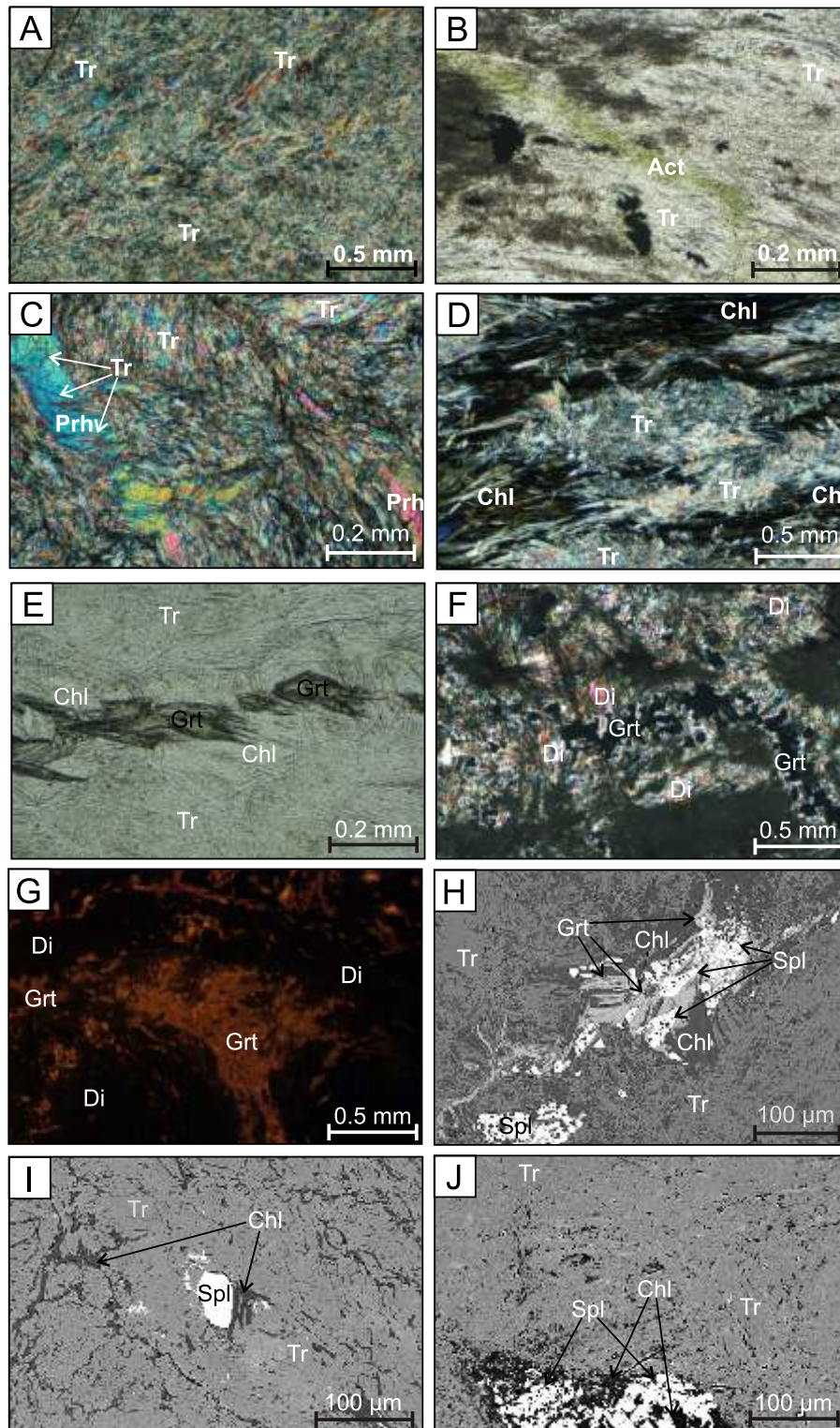


Fig. 4. Thin-section photomicrographs under plane-polarized light (B, E) and cross-polarized light (A, C, D, F), cathodoluminescence photomicrograph (G), and back-scattered electron (BSE) images (H–J) of Jordanów nephrite

A – nephrite tremolite groundmass; **B** – green actinolite vein cutting colourless tremolite nephrite; **C** – tremolite needles formed at the expense of prehnite (tremolite replacing prehnite veins); **D** – nephrite (tremolite) nests formed at the expense of chlorite schist; **E** – vein composed of garnet mantled by chlorite in nephrite; **F** – acicular fan-shaped diopside aggregates and garnet veins; **G** – bright orange to yellow cathodoluminescent garnets; **H** – aggregate composed of Cr-spinel and garnet cores mantled by chlorite; **I** – Cr-spinel with chlorite mantle; **J** – dismembered and altered spinel with chlorite rim; Act – actinolite, Chl – chlorite, Di – diopside, Grt – garnet, Prh – prehnite, Spl – spinel, Tr – tremolite

phases, in both nephrite and nephrite schist, are antigorite, hydrogrossular, zircon, apatite and monazite (Gil, 2013).

Nephrite tremolite groundmass contains relics of diopside, chlorite, and garnet; some larger diopside porphyroblasts are rotated and cataclased, and have chlorite-tremolite pressure shadows. Some, partly-replaced by tremolite chlorite nests, show interlocking non-pseudomorphic textures (Gil, 2013). Our present study reveals rare, green, secondary actinolite veins cutting colourless tremolite groundmass in Jordanów nephrite (Fig. 4B). Prehnite veins cutting nephrite schist groundmass, composed of tremolite and diopside, are then replaced by secondary, automorphic tremolite needles (Fig. 4C). Secondary tremolite, replacing prehnite veins can be isochronous with secondary actinolite veins. In some places, prehnite veins are completely replaced by the secondary tremolite. Tremolite usually replaces diopside (tremolite overgrowing diopside), although in places tremolite (nephrite) nests within chlorite schist form at the expense of chlorites (Fig. 4D). Automorphic tremolite porphyroblasts are present, although automorphic diopside is very rare; it is usually cataclased and partly replaced by tremolite. Automorphic garnet crystals are more common, although the majority of the garnets are rotated (locally with chlorite pressure shadows), elongated or are overgrown by chlorite, tremolite, and Cr-spinel. Some grossular garnets occur as crystals mantled by chlorite (Fig. 4E); other garnet aggregates are vein-shaped or occur with acicular fan-shaped diopside aggregates (rodingite relics; Fig. 4F). Garnets' cathodoluminescence is yellow, bright orange or orange (Fig. 4G). Cr-spinels occur as dismembered and altered aggregates or single crystals, with chlorite intergrowths and rims (Fig. 4H, I, J). Within spinel-chlorite aggregates, elongated garnet relics are present (Fig. 4H).

According to Lobos et al. (2008), some of the Nasławice nephrite samples show homogeneous surfaces, whereas others are spotted (black spots) or patchy. Its transparency varies from semitranslucent to opaque. The nephrite's colour is white, green, dark green or emerald-green, and its polished surface luster is vitreous or greasy. The rock is composed of tremolite-actinolite amphiboles (size 20–100 µm), diopside, Cr-garnet, and Cr-spinel (garnet usually has amphibole and Cr-spinel overgrowths; Lobos et al., 2008).

The Crooks Mountain nephrite, examined in the present study, is opaque with minor semitranslucent zones, and bright to dark green, with minor white and creamy elongated vein-like zones. The polished surface is chaotic, layered or spotted (black opaque spinel spots). The luster is dull, waxy, greasy or sub-vitreous. The specimen analysed, based on petrology, modal mineralogy, and its fabric, is identified as a nephrite-schist (also semi-nephrite). It is composed of actinolite (60.11 vol.%), diopside (33.74 vol.%), chlorite (4.75 vol.%), and opaque minerals (Cr-spinel and heazlewoodite; 1.41 vol.%). Accessory phases are Cr-garnet, hydrogrossular, and titanite. Actinolite needles are between ~10 and 50 µm in length.

The New Zealand nephrite specimen is semitranslucent with an intense green to dark green colour. Its polished surface is either homogeneous or spotted (black opaque spinel spots), and it has a waxy to greasy luster. The specimen is a nephrite *sensu stricto* and is composed of tremolite (87.46 vol.%), chlorite (12.19 vol.%), and opaque minerals (Cr-spinel and heazlewoodite; 0.35 vol.%). The tremolite needles are ca. 10–60 µm in length.

MINERAL CHEMISTRY

The Jordanów nephrite amphibole is tremolite with Si between 7.73 and 7.99 apfu, Mg/(Mg + Fe²⁺) from 0.90 to 0.94, 0.02–0.32 wt.% Cr₂O₃, and 0.03–0.28 wt.% NiO (Appendix 1*). Diopside is composed of 47–51 wollastonite (Wo), 41–48 enstatite (En), and 3–9 ferrosilite (Fs), and contains 0.00–0.51 wt.% Cr₂O₃ and 0.00–0.09 wt.% NiO. In the present study, we divided chlorites to “chlorite I” and “chlorite II”, representing primary chlorite forming black-wall, and secondary chlorite formed as a result of rodingite garnet decomposition, respectively. Previously studied (Gil, 2013) chlorites (cf. “chlorite I” and subordinate “chlorite II”) have Si (IV) between 2.92 and 3.58, Fe²⁺/Sum R²⁺ from 0.06 to 0.28, and contain 0.00–0.87 wt.% Cr₂O₃. We analysed chlorite rims around spinel crystals (“chlorite II”), which have the following composition: Si (IV) 2.84–3.14, Fe²⁺/Sum R²⁺ from 0.10 to 0.12, and Cr₂O₃ from 1.37 to 4.41 wt.%. Garnet has Ca/(Ca + Mg) between 0.96 and 1.00, Mg/(Mg + Fe) ratios from 0.03 to 0.73 and contains 0.01–1.20 wt.% Cr₂O₃. Spinel (also spinel cores surrounded by chlorite rims) are composed of: MgO (0.68–1.96 wt.%), FeO (24.87–27.91 wt.%), Fe₂O₃ (8.72–16.49 wt.%), Al₂O₃ (3.53–4.36 wt.%), and Cr₂O₃ (46.74–54.46 wt.%). Apatite has Ca between 39.26 and 40.38 wt.%, and P between 18.25 and 18.96 wt.% (Appendix 1).

Lobos et al. (2008) describe the Nasławice nephrite amphibole as actinolite, although according to the Leake et al. (1997) classification, some samples contain tremolite, rather than actinolite (Fig. 5). Amphiboles have 7.85–7.94 Si apfu and 0.82–0.92 Mg/(Mg + Fe²⁺), and contain 0.26–0.94 wt.% Cr₂O₃ and 0.08–0.21 wt.% NiO (Appendix 1). Clinopyroxene (diopside) is composed of 50–51 Wo, 44–45 En, and 5–6 Fs, and contains 0.20–0.83 wt.% Cr₂O₃ and 0.06–0.08 wt.% NiO. Garnet has Ca/(Ca + Mg) ~1.00, Mg/(Mg + Fe) ratio from 0.01 to 0.04 and contains 14.37–15.13 wt.% Cr₂O₃. Spinel is composed of: MgO (0.29–0.51 wt.%), FeO (29.40–29.67 wt.%), Fe₂O₃ (20.70–22.82 wt.%), Al₂O₃ (3.11–3.27 wt.%), and Cr₂O₃ (39.07–41.00 wt.%; Lobos et al., 2008).

The Crooks Mountain nephrite actinolite has 7.76–8.03 Si apfu, 0.86–0.90 Mg/(Mg + Fe²⁺), and contains 0.02–0.11 wt.% Cr₂O₃ (Appendix 2). Diopside is composed of 47–51 Wo,

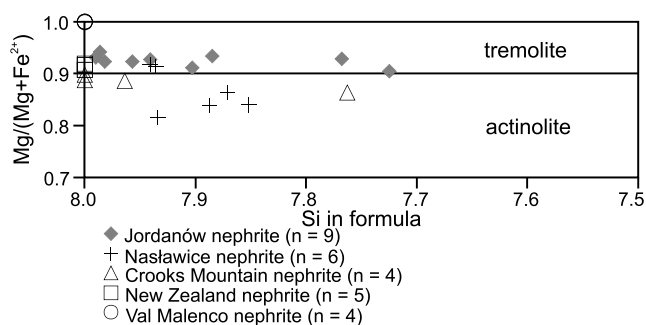


Fig. 5. The GJM nephrites (Jordanów and Nasławice quarries, Gil, 2013; Lobos et al., 2008, respectively) amphiboles composition compared with the serpentine-related Crooks Mountain (the Granite Mountains, Wyoming, USA) and New Zealand nephrites amphiboles (this study), and with the dolomite-related Val Malenco nephrite amphibole (Italy; Adamo and Bocchio, 2013); classification diagram after Leake et al. (1997)

* Supplementary data associated with this article can be found, in the online version, at doi: 10.7306/gq.1228

41–48 En, and 5–9 Fs, and contains 0.02–0.64 wt.% Cr₂O₃ and 0.00–0.11 wt.% NiO. Chlorite has Si (IV) between 3.10 and 3.35 apfu, Fe²⁺/Sum R²⁺ from 0.15 to 0.18, and Cr₂O₃ from 0.67 to 6.34 wt.%. Garnet has Ca/(Ca + Mg) from 0.92 to 0.98, Mg/(Mg + Fe) ratio from 0.20 to 0.61, and Cr₂O₃ from 14.10 to 16.43 wt.%. Spinels are composed of MgO (7.02–14.90 wt.%), FeO (13.85–22.26 wt.%), Fe₂O₃ (2.15–5.81 wt.%), Al₂O₃ (10.88–35.91 wt.%), and Cr₂O₃ (30.52–58.05 wt.%).

The New Zealand nephrite tremolite has 8.00–8.05 Si apfu, 0.91–0.92 Mg/(Mg + Fe²⁺), and contain 0.05–0.13 wt.% Cr₂O₃ (Appendix 2). Chlorite has Si (IV) between 2.99 and 3.07, Fe²⁺/Sum R²⁺ from 0.14 to 0.15, and contains 0.48 to 5.33 wt.% Cr₂O₃. Spinels are composed of MgO (9.97–11.72 wt.%), FeO (14.67–17.48 wt.%), Fe₂O₃ (1.61–3.01 wt.%), Al₂O₃ (5.92–20.77 wt.%), and Cr₂O₃ (47.48–65.68 wt.%).

BULK-ROCK CHEMICAL COMPOSITION

The bulk-rock composition of the Jordanów nephrite (PGAA; in wt.%) is: 56.70 SiO₂, 0.0048 TiO₂, 2.33 Al₂O₃, 3.89 Fe₂O₃, 0.127 MnO, 21.30 MgO, 12.40 CaO, 0.05 Na₂O, <0.02 K₂O, 2.84 H₂O, <0.05 SO₃, and <0.50 As₂O₃. Trace elements concentrations (in ppm) are as follows: 1.6 B, <10 Cl, <40 V, 1220 Cr, 47 Co, 1408 Ni, <5 Nd, <0.5 Sm, <0.5 Gd; Fe/(Fe + Mg) ratio 0.084 (cf., Table 2; Péterdi et al., 2014).

According to Kostov et al. (2012), the bulk composition of the Jordanów nephrite (by means of proton microbeam particle-induced X-Ray emission, micro-PIXE) is (in wt.%): 56.63 SiO₂, <0.0025 TiO₂ (detection limit recalculated from ppm Ti), 0.98 Al₂O₃, 4.61 Fe₂O₃ (recalculated from FeO), 0.029 MnO, 22.82 MgO, 13.39 CaO, 0.03 Na₂O, <0.01 SO₃ (detection limit recalculated from ppm S); trace elements (in ppm): 178 P, <35 Cl, 86 V, 719 Cr, 260 Co, 1623 Ni, 4 Cu, 84 Zn; calculated Fe/(Fe + Mg) ratio 0.093 (Table 2).

OXYGEN AND HYDROGEN ISOTOPE COMPOSITION

The nephrite schist's H isotope composition was not analysed to avoid mixed signals of tremolite and chlorite (high chlorite amounts in nephrite schist). Nephrite schist O isotope analysis was duplicated to ensure that chlorite did not affect the δ¹⁸O value (analyses duplicate well). Jordanów nephrite and nephrite schist δ¹⁸O values are +6.1‰ (n = 1) and +6.7‰ (n = 2), respectively (Table 3). The nephrite δD value is –61‰ (n = 2; Table 3).

Table 3

Oxygen and hydrogen isotope composition of Jordanów nephrite and nephrite schist relative to SMOW

Analyse no	Sample	δ ¹⁸ O ‰	δD‰
1	nephrite	6.1 ^{a, c}	-61 ^{b, d}
2	nephrite schist	6.7 ^{a, c, d}	

a – analysed in the Jackson School of Geosciences, the University of Texas at Austin, United States; b – analysed in the Institute for Geosciences and Earth Resources, the National Research Council of Italy in Pisa; c – error ±0.1‰; d – average value from 2 analyses

DISCUSSION

SERPENTINITE-RELATED ORIGIN

The Jordanów nephrite can be divided into nephrite *sensu stricto* and nephrite schist (semi-nephrite). The nephrite *sensu stricto* composition (87.2–89.8 vol.% amphiboles, 4.7–5.7 vol.% diopside, 3.8–8.1 vol.% chlorites, up to 0.2 vol.% Cr-spinels, and up to 0.5 vol.% garnets) corresponds with New Zealand nephrite (87.46 vol.% amphiboles, 12.19 vol.% chlorite, and 0.35 vol.% Cr-spinel and heazlewoodite). All known New Zealand nephrites are interpreted as serpentinite-related (Middleton, 2006; Adams et al., 2007). The Jordanów nephrite schist composition (33.5–79.7 vol.% amphiboles, 7.4–55.1 vol.% diopside, 5.0–38.9 vol.% chlorites, up to 4.2 vol.% Cr-spinels, up to 10.8 vol.% garnets, up to 0.5 vol.% prehnite, up to 0.8 vol.% titanite, up to 9.7 vol.% clay minerals-oxides aggregates, accessory e.g., hydrogrossular) corresponds with the nephrite-schist (semi-nephrite) from Crooks Mountain (60.11 vol.% amphiboles, 33.74 vol.% diopside, 4.75 vol.% chlorite, 1.41 vol.% Cr-spinel and heazlewoodite, accessory Cr-garnet, hydrogrossular garnet and titanite), which is also interpreted as serpentinite-related (Middleton, 2006).

The Jordanów nephrite contains solely tremolite, whereas the Naślawice nephrite contains both actinolite and tremolite (Fig. 5). Hence, the Naślawice nephrite amphiboles are slightly Fe-enriched compared to Jordanów nephrite amphibole, although both the GJM nephrites have Fe contents in amphiboles, comparable with the serpentinite-related Crooks Mountain and New Zealand nephrite amphiboles. The amphiboles in GJM nephrites have similar Si apfu (7.73–7.99) to those from Crooks Mountain (Si apfu = 7.76–8.03). The amphibole Mg/(Mg + Fe²⁺) ratio (0.82–0.94) is also similar to those of Crooks Mountain (0.86–0.90) and New Zealand (0.91 to 0.92) nephrite amphiboles. Most of the GJM samples contain amphiboles that have lower Si apfu and Mg/(Mg + Fe²⁺) ratios than those reported from the dolomite-related Val Malenco nephrite (Italy) amphibole, which has Si apfu ~8.0 and Mg/(Mg + Fe²⁺) ~1.0 (Fig. 5; Adamo and Bocchio, 2013). However, there is an overlap in several samples, cf., 7.99 and 8.0 Si apfu. The Cr₂O₃ content in the GJM nephrite amphiboles (0.02–0.94 wt.%) is more similar to the serpentinite-related nephrite amphiboles (0.02–0.43 wt.%), rather than to the majority of the dolomite-related nephrite amphiboles (0.00–0.09 wt.%; Liu et al., 2011a; Ling et al., 2013), although there are several dolomite-related nephrites with elevated Cr₂O₃ in amphiboles (0.03–1.18 wt.%; cf., Table 1). Also, the GJM nephrite amphiboles' NiO content (0.03–0.28 wt.%) is more similar to the serpentinite-related amphiboles (0.08–0.36 wt.%), rather than to dolomite-related (0.00–0.08 wt.% NiO) type amphiboles (cf., Grapes and Yun, 2010; Liu et al., 2011a; Ling et al., 2013), although there is some overlap.

The diopside composition (Morimoto et al., 1988) of the GJM nephrites (Fig. 6A) is more similar to the serpentinite-related Crooks Mountain nephrite diopside (Fig. 6B) than to the dolomite-related Hetian (Liu et al., 2011a) and Alamas (Liu et al., 2011b) nephrite diopsides (both Xinjiang, NW China; Fig. 6C). The wollastonite component in diopside in the GJM nephrite varies from the maximum amount (51 Wo) to close to augite (47 Wo), similar to the Crooks Mountain diopside (47–51 Wo; Fig. 6A, B). The ferrosilite component (3–9 Fe) is similar to the Crooks Mountain diopside (5–9 Fe), and higher than in dolomite-related Chinese nephrite diopsides (1–6 Fe; Fig. 6C). The

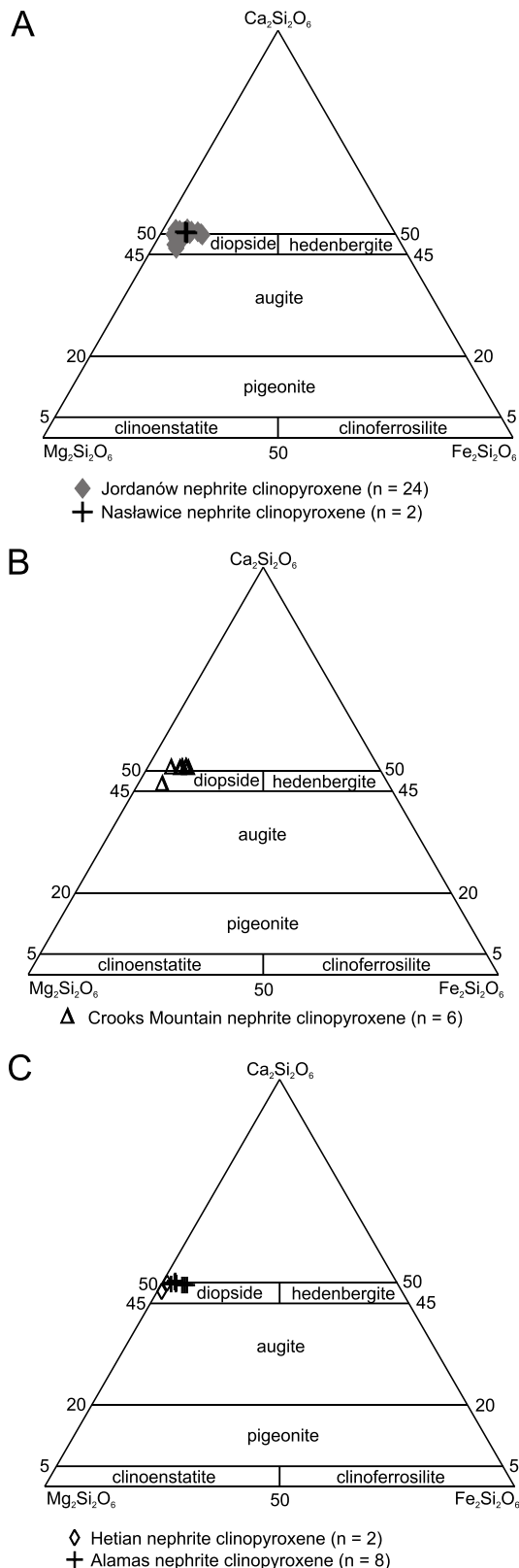


Fig. 6. The GJM (Jordanów and Nasławice quarries; Lobos et al., 2008; Gil, 2013, respectively), Crooks Mountain (this study), and Hetian and Alamas (both Xinjiang, China) nephrite clinopyroxene composition: A – Jordanów and Nasławice nephrites, B – Crooks Mountain serpentinite-related nephrite, C – Hetian (Liu et al., 2011a) and Alamas (Liu et al., 2011b) dolomite-related nephrites; classification diagram after Morimoto et al. (1988)

diopside in the GJM samples has Cr₂O₃ concentrations (0.00–0.83 wt.%) similar to the serpentinite-related Crooks Mountain nephrite diopside (0.02–0.64 wt.%), in contrast to those in the dolomite-related Alamas nephrite diopside (0.00–0.03 wt.%; Liu et al., 2011b), but with some overlap.

The Jordanów nephrite apatite composition, presented as the variation of P (wt.%) vs. Ca (wt.%) diagram (Kuroda et al., 2005), differs from the dolomite-related Hetian nephrite apatite (Liu et al., 2011a) – the Jordanów samples are slightly enriched in Ca (Fig. 7). The difference may be due to a serpentinite-related origin or to different P–T conditions during crystallisation.

In the Jordanów nephrite, chlorite rims around spinel crystals (“chlorite II”; clinochlore and subordinate penninite) are similar in composition to chlorites from chlorite schists in Ronda peridotites in Spain (major population plots as clinochlore, brunsvigite and ripidolite, with subordinate penninite and sherdanite; Esteban et al., 2007), from which serpentinite-related nephrites were also described (Cuevas et al., 2006). Additionally, the “chlorite II” is also similar in composition to spinel chlorite rims from the New Zealand serpentinite-related nephrite (Fig. 8).

Garnets from the GJM nephrites plot within the crustal-derived garnets field (Fig. 9), which implies a possible genetic relationship with leucogranite rodingitisation. The Fengtien serpentinite-related nephrite (Wan and Yeh, 1984) and Crooks Mountain serpentinite-related nephrite garnets also plot in the crustal-derived garnets field (Fig. 9). In addition, the garnet in the Nasławice nephrite is Mg-depleted [0.01–0.04 Mg/(Mg + Fe)] relative to that from the Jordanów nephrite [0.03–0.73 Mg/(Mg + Fe)]. The garnet in the Nasławice samples is also more abundant in Cr (14.37–15.13 wt.% Cr₂O₃) and less abundant in Al (3.04–4.05 wt.% Al₂O₃) in comparison to garnet from Jordanów samples (0.01–1.20 wt.% Cr₂O₃ and 20.82–22.32 wt.% Al₂O₃). Hence, the composition of garnets in nephrite can vary significantly within the deposit; Cr content dramatic rises and Al drops at the distance of ca. 2 km towards NW, from Jordanów to Nasławice Quarry.

The bulk-rock major element composition of the Jordanów nephrite also supports a serpentinite-related origin. The variation of FeO (ppm) vs. Fe/(Fe + Mg) (Siqin et al., 2012) of the two Jordanów nephrite analyses (performed by different methods – the prompt-gamma activation analysis, PGAA; Péterdi et al.,

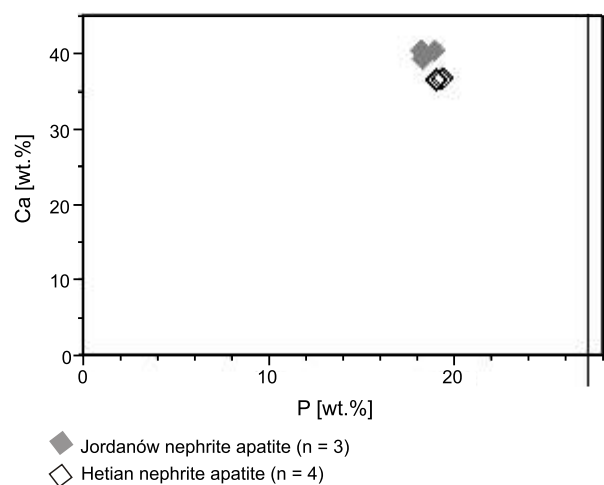


Fig. 7. Jordanów nephrite (Gil, 2013) and dolomite-related Hetian nephrite (Liu et al., 2011a) apatites composition presented on P (wt.%) vs. Ca (wt.%) diagram after Kuroda et al. (2005)

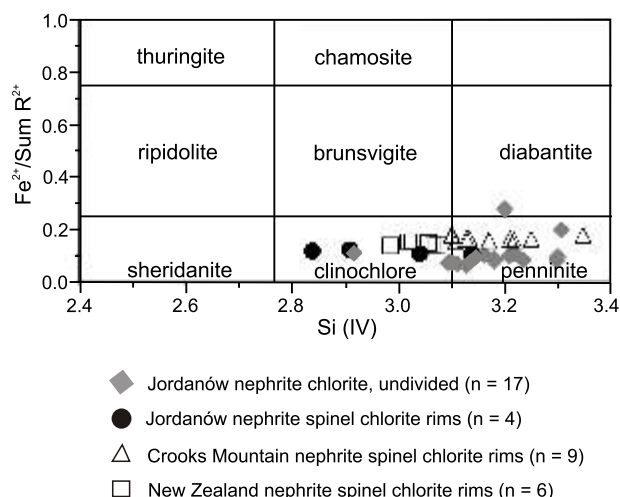


Fig. 8. Jordanów nephrite chlorites (chlorite rims on spinels – “chlorite II”, this study; and previously reported data on undivided chlorites – “chlorite I” and subordinate “chlorite II”, Gil, 2013) compared with chlorite rims on spinels from the serpentinite-related Crooks Mountain and New Zealand nephrites (this study) on Foster’s diagram (1962, fide Esteban et al., 2007)

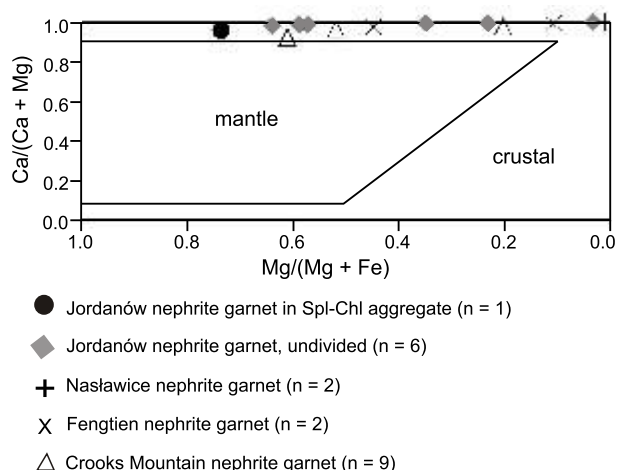


Fig. 9. Garnets from the Jordanów (garnet relict within spinel-chlorite aggregate, this study, and previously published undivided garnet, Gil, 2013) and Nastawice (Łobos et al., 2008) nephrites comparison with garnets from serpentinite-related Fengtien (Taiwan; Wan and Yeh, 1984) and Crooks Mountain (this study) nephrites on Schulze’s (2003) discrimination diagram; Chl – chlorite, Spl – spinel

2014, and the proton microbeam particle-induced X-Ray emission, micro-PIXE; Kostov et al., 2012) show that the nephrite plots in the serpentinite-related nephrites field, regardless of analytical method (Fig. 10). The Fe/(Fe + Mg) ratios of 0.084 and 0.093 are similar to the serpentinite-related nephrite type values proposed by Siqin et al. (2012) – the Fe/(Fe + Mg) ratios above 0.060. In addition, the bulk-rock trace elements also correspond with the serpentinite-related nephrites, based on Cr and Ni concentrations (Fig. 11). In the Jordanów nephrite, Cr

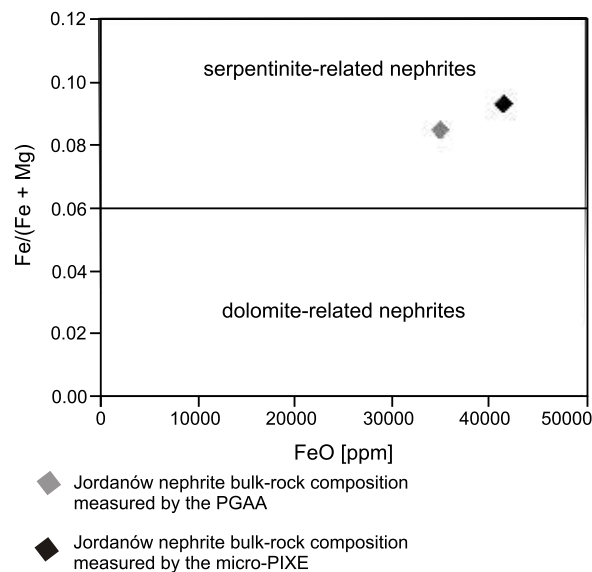


Fig. 10. Jordanów nephrite bulk-rock chemical composition performed by different methods (i.e., prompt-gamma activation analyse, PGAA, Péterdi et al., 2014, and proton microbeam particle-induced X-Ray emission, micro-PIXE, Kostov et al., 2012) on discrimination diagram after Siqin et al. (2012)

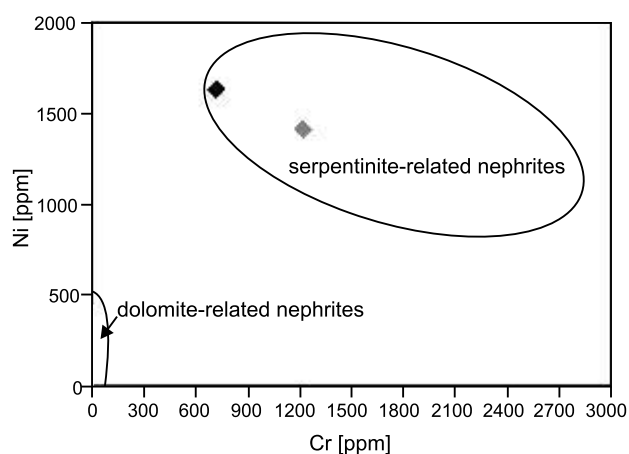


Fig. 11. Jordanów nephrite bulk-rock Cr and Ni on discrimination diagram modified after Adamo and Bocchio (2013); the dolomite-related and serpentinite-related nephrite fields based on analyses by means of glow discharge mass spectrometry (GD-MS) after Siqin et al. (2012), and proton microbeam particle-induced X-Ray emission (micro-PIXE) after Kostov et al. (2012)

For other explanations see Figure 10

(719 and 1220 ppm) is more similar to that of the serpentinite-related nephrites (900–2812.1 ppm Cr), rather than that of the dolomite-related ones (1.9–178.7 ppm Cr). The bulk-rock Ni (1408 and 1623 ppm) is typical of the serpentinite-related samples (958.7–1898 ppm Ni) and much higher than in the dolomite-related type (0.05–470.7 ppm Ni; cf., Table 1). The serpentinite-related nephrites bulk-rock Co concentration is usually higher than that of the dolomite-related samples (Middleton 2006 and references therein). The Jordanów nephrite bulk-rock

analyses show 47–260 ppm Co, depending on method (Table 2), which is similar to serpentinite-related nephrites from China, Siberia, New Zealand, and Canada (42–207 ppm Co; Kostov et al., 2012; Siqin et al., 2012, recalculated), and higher than of the dolomite-related nephrites from China (0.5–9.8 ppm Co; Siqin et al., 2012, recalculated).

The nephrite and nephrite schist $\delta^{18}\text{O}$ values (+6.1 to +6.7 \pm 0.1‰) in Jordanów samples correspond with published data from the serpentinite-related nephrites elsewhere (+4.5 to +9.6‰), although they overlap with the upper limit of the dolomite-related nephrites (–9.9 to +6.2‰; Yui et al., 1988; Yui and Kwon, 2002; Liu et al., 2011a, b). The Jordanów nephrite and nephrite schist $\delta^{18}\text{O}$ values are higher than the published $\delta^{18}\text{O}$ values of OH groups of serpentines from Jordanów (–6.3 to +1.6‰) and Nasławice (–7.8‰; J drysek et al., 1991). The nephrite δD value (–61‰) corresponds with the lower limit of the published serpentinite-related nephrites (–67 to –33‰; Yui et al., 1988; Yui and Kwon, 2002), although they also overlap with the dolomite-related type upper limit (–124 to –55.7‰; Yui and Kwon, 2002; Liu et al., 2011a, b; Adamo and Bocchio, 2013). The Jordanów nephrite δD value is lower than in the serpentines from Jordanów (–48.5 to –40.3‰) and Nasławice (–96.8‰ and –46.3 to –43.1‰; J drysek et al., 1991). However, the lowest δD value of the serpentines from Nasławice probably reflects late stage interaction with meteoric water, unrelated to the nephrite formation. It should be noted that in case of nephrite, similar oxygen and hydrogen isotope compositions do not necessarily reflect similar origins (cf., Yui and Kwon, 2002; Liu et al., 2011a), as isotopic compositions may vary due to fluid source, temperature of formation, and water/rock ratio. However, when plotted in diagram $\delta^{18}\text{O}$ vs. δD , modified after Yui and Kwon (2002) and Liu et al. (2011a, b), the Jordanów nephrite corresponds with data published for the serpentinite-related nephrites, although it plots not far from several dolomite-related nephrites (Fig. 12).

CRYSTALLIZATION STAGES

Four crystallisation stages in the Jordanów nephrites are proposed, based on microscopic observations, including data available from other nephrite deposits. The first crystallisation stage, prior to nephrite formation, was rodingitisation: granite was replaced by rodingite mineral paragenesis (diopside and garnet; see Fig. 4F), and chlorite black-wall (“chlorite I”) was formed at the rodingite contact. The second stage was nephritisation: tremolite (“tremolite I”) formed at the expense of diopside within rodingite and at the expense of “chlorite I” within chlorite black-wall (see Fig. 4D), garnet breakdown into chlorite (“chlorite II”), and spinel (see Fig. 4E, H–J). The third crystallisation stage was the formation of prehnite veins (see Fig. 4C). The fourth crystallisation stage was a secondary amphibole formation, replacing the prehnite veins with tremolite (“tremolite II”; see Fig. 4C) and the formation of actinolite veins (see Fig. 4B).

Diopside recrystallisation to tremolite is one of the major mechanisms of nephrite formation (e.g., Liu et al., 2011a, b). Chlorite (e.g., Devine et al., 2007) and spinel (e.g., Dubińska et al., 2004; De Hoog et al., 2009) are common products of garnet breakdown. However, chlorite rims around spinel crystals (“chlorite II”) can also form due to the metamorphic reaction of spinel with serpentine minerals above 400°C (the upper-greenschist facies), documented in numerous chromitite bodies (Derbyshire et al., 2013 and references therein). The GJM

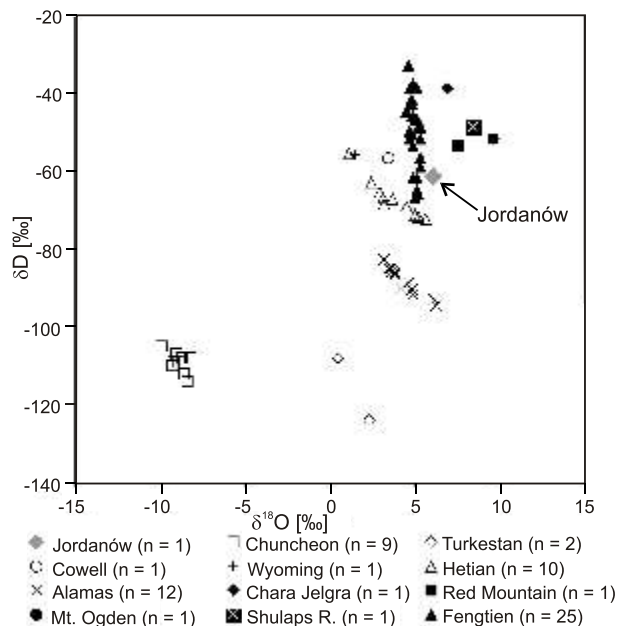


Fig. 12. Jordanów nephrite (this study) stable isotope composition, compared with published serpentinite-related nephrites (solid symbols; Chara Jelgra River, Red Mountain, Mt. Ogden and Shulaps Range, all after Yui and Kwon, 2002, and Fengtien after Yui et al., 1988) and dolomite-related nephrites (open symbols; Chuncheon, Turkestan, Cowell, Wyoming, all after Yui and Kwon, 2002, Hetian, after Liu et al., 2011a, and Alamas, after Liu et al., 2011b); diagram modified after Yui and Kwon (2002) and Liu et al. (2011a, b); we note that the Wyoming sample plotted here is a dolomite-related nephrite, as opposed to the serpentinite-related Wyoming sample studied in this contribution

nephrite spinels presented on the discrimination diagram (modified after Proenza et al., 2004; Barkov et al., 2009 and references therein; Fig. 13) show variable compositions – chromite with increasing magnetite content and constant Al (3.11–4.36 wt.% Al_2O_3). The least abundant in Fe^{3+} are spinel crystals surrounded by chlorites (garnet break-down products, second crystallisation stage) from Jordanów. In contrast, spinel from Nasławice has the most Fe^{3+} . The spinels with the lowest Fe^{3+} contents likely formed during greenschist facies metamorphism. Hence, spinels composition suggests that the second stage of nephrite formation occurred under greenschist-facies conditions, although lower-amphibolite-facies cannot be excluded. Another explanation of the formation of the chlorite rims around spinel crystals (“chlorite II”; spinel with serpentine minerals reaction in temperatures above 400°C) also correlates the second nephrite crystallisation stage with upper-greenschist or lower-amphibolite-facies conditions. Figure 13 shows that spinels from Crooks Mountain and New Zealand nephrites are more Al-abundant and less Fe^{3+} -abundant than the GJM nephrite spinels. The Crooks Mountain and New Zealand nephrites spinels plot in the greenschist-facies and lower-amphibolite-facies fields, and the minerals from the same specimen can plot in both fields.

Most chlorites (“chlorite I”, subordinate “chlorite II”) from the Jordanów nephrite are penninite, with subordinate clinocllore and diabantite (Fig. 8; Gil, 2013). Some chlorite rims around spinel crystals (“chlorite II”) are clinocllore and minor penninite (see Fig. 8). Hence, spinel chlorite rims (“chlorite II”) contain

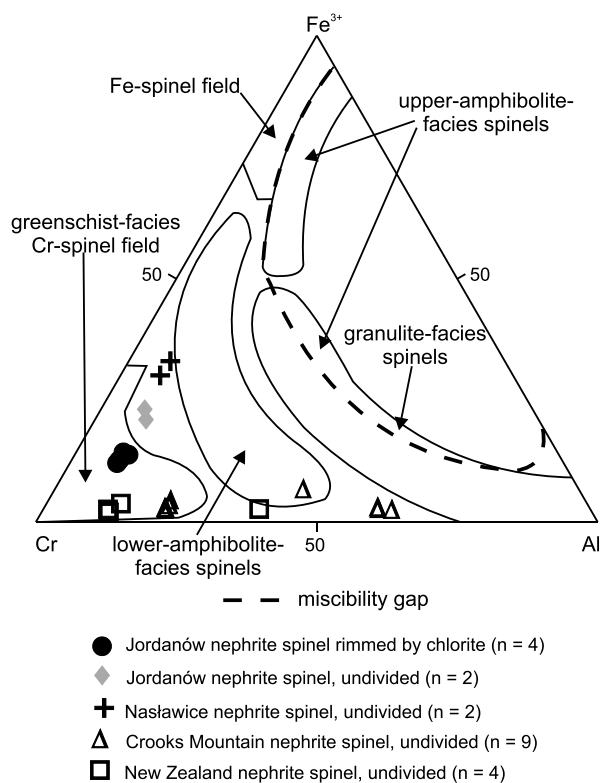


Fig. 13. Spinel from the Jordanów (spinel rimmed by chlorite, this study, and undivided spinel, after Gil, 2013), Naślawice (undivided spinel, after Łobos et al., 2008), Crooks Mountain and New Zealand nephrites (this study) on discrimination diagram modified after Proenza et al. (2004) and Barkov et al. (2009) and references therein

less Si (IV) – 2.84–3.14 (29.16–31.89 wt.% SiO₂), compared to the major chlorite population (“chlorite I”, subordinate “chlorite II”): Si (IV) – 2.92–3.58 (30.94–38.56 wt.% SiO₂). In addition, the chlorite rims around spinel crystals (“chlorite II”) have higher Cr concentrations (1.37–4.41 wt.% Cr₂O₃) than the major chlorite population (“chlorite I”, subordinate “chlorite II”); 0.00–0.87 wt.% Cr₂O₃).

An assignment of the exact ages to the crystallisation stages is problematic. Black-wall around rodingite formation in Naślawice is dated based on zircon inclusions U-Pb age to 400 ± 4/–3 Ma (Dubinska et al., 2004), which can be correlated with the first crystallisation stage (black-wall in Jordanów composed of “chlorite I”). A partially-rodingitised leucogranite vein, adjacent to the contact zone (black-wall) from which most of the examined nephrite samples were extracted, contains zircon dated with the U-Pb SHRIMP method to 337 ± 4 Ma (main zircon population; Kryza, 2011), hence, this age can also be correlated with the first crystallisation stage.

SUMMARY AND CONCLUSIONS

We show that the GJM nephrites are of serpentinite-related origin (ortho-nephrite), which is confirmed by the mineralogical and geochemical data obtained using various analytical techniques. The Jordanów nephrite *sensu stricto* and nephrite

schist (semi-nephrite) compositions are similar to the serpentinite-related nephrites from Crooks Mountain and New Zealand. Amphiboles from the GJM nephrite contain 0.02–0.94 wt.% Cr₂O₃, similar to the serpentinite-related nephrite amphiboles (0.02–0.43 wt.% Cr₂O₃), rather than to the dolomite-related variety amphiboles (0.00–0.09 wt.% Cr₂O₃). The NiO contents (0.03–0.28 wt.%) are also more similar to the serpentinite-related nephrite amphiboles (0.08–0.36 wt.% NiO), than to the dolomite-related type amphiboles (0.00–0.08 wt.% NiO).

The diopside from the GJM nephrites is compositionally more similar to the serpentinite-related Crooks Mountain nephrite diopside, than to the dolomite-related Hetian and Alamas nephrites diopside. The GJM nephrites diopside contain high Cr₂O₃ contents (0.00–0.83 wt.%), similar to the serpentinite-related Crooks Mountain nephrite diopside (0.02–0.64 wt.% Cr₂O₃), and different from the consistently low Cr₂O₃ concentrations in the dolomite-related Alamas nephrite diopside (0.00–0.03 wt.% Cr₂O₃). In addition, the Jordanów nephrite apatite contains more Ca compared to the dolomite-related Hetian nephrite apatite.

The chlorite rims around spinel crystals (“chlorite II”; clinocllore and subordinate penninite) in the Jordanów nephrite are similar to the important population of chlorites (clinocllore, brunsvigite, ripidolite, and subordinate penninite and sherdanite) from chlorite schists of the Ronda peridotites (one of the largest orogenic Iherzolite bodies in the world, located in Spain, serpentinitised, containing rodingite, gabbro, granite, and chlorite schist bodies; cf. Cuevas et al., 2006; Esteban et al., 2007), associated with the serpentinite-related nephrites. The chlorite rims (“chlorite II”) are also similar to spinel crystals chlorite rims (clinocllore) from the New Zealand serpentinite-related nephrite. The GJM nephrites garnets are crustal-derived, similar to garnets from the Fengtien and Crooks Mountain serpentinite-related nephrites. Interestingly, the garnet from Naślawice nephrite is Mg- and Al-depleted (0.01–0.04 Mg/(Mg + Fe) and 3.04–4.05 wt.% Al₂O₃) and Cr-enriched (14.37–15.13 wt.% Cr₂O₃), relative to the Jordanów nephrite garnet (0.03–0.73 Mg/(Mg + Fe), 20.82–22.32 wt.% Al₂O₃ and 0.01–1.20 wt.% Cr₂O₃), which shows that the garnets composition can vary significantly within a given nephrite occurrence.

The Jordanów nephrite has high bulk-rock Fe/(Fe + Mg) ratios, corresponding to the serpentinite-related nephrites. The bulk-rock Cr, Ni, and Co are also typical of the serpentinite-related nephrites and higher than in the dolomite-related varieties. The measured concentrations are similar to the serpentinite-related nephrites regardless of the analytical method used, whether that be prompt-gamma activation analysis (PGAA) or proton microbeam particle-induced X-Ray emission (micro-PIXE).

The nephrite and nephrite schist from Jordanów have δ¹⁸O values ranging from +6.1 to +6.7‰, and the average nephrite δD value is –61‰. The average δD value is lower than the δD values of most serpentine samples from the host-rocks. The nephrite δ¹⁸O and δD correspond with the published data on the serpentinite-related nephrites, although they plot not far from several dolomite-related specimens.

According to the observed mineral paragenesis in the GJM nephrites, four crystallization stages are proposed:

- leucogranite rodingitisation (diopside and garnet) and chlorite black-wall (“chlorite I”) formation;
- nephritisation – tremolite (“tremolite I”) after diopside in rodingite and after “chlorite I” in chlorite black-wall; spinel and chlorite (“chlorite II”) formed as a result of garnet breakdown, although “chlorite II” can be formed in the way of spinel with serpentines reaction;

- prehnite veins formation;
- tremolite (“tremolite II”) after prehnite veins, actinolite veins formation.

Further studies can precisely identify proposed crystallisation stages.

The spinels composition in the GJM nephrites suggests, at least for the second crystallisation stage, greenschist-facies conditions, although lower-amphibolite-facies is not excluded. The chlorite rims around spinel crystals (“chlorite II”) contain less Si (IV): 2.84–3.14 apfu (29.16–31.89 wt.% SiO₂), and more Cr (1.37–4.41 wt.% Cr₂O₃), relative to the major chlorites population in nephrite (“chlorite I”, subordinate “chlorite II”) – Si (IV): 2.92–3.58 (30.94–38.56 wt.% SiO₂) and 0.00–0.87 wt.% Cr₂O₃. The chlorite rims around spinel crystals (“chlorite II”) seems to have elevated Cr inherited from the garnet or spinel, unlike chlorite black-wall (“chlorite I”), which is less abundant in Cr, due to the lack of an abundant source.

The first crystallisation event can be tentatively assigned to either the zircon age from rodingite black-wall in Naślawice (400 ± 4–3 Ma; [Dubiska et al., 2004](#)), or the zircon age from partially-rodingitized leucogranite in Jordanów (337 ± 4 Ma; [Kryza, 2011](#)). Detailed timing of the crystallisation stages requires further investigation.

Acknowledgements. The research has been supported by the University of Wrocław – Institute of Geological Sciences, and Eötvös Loránd University – Institute of Geography and Earth Sciences internal grants and partially supported by the Project “Development of the potential and educational offer of the University of Wrocław – the chance to enhance the competitiveness of the University” co-financed by the European Union under the European Social Fund. J. Girulski-Michalik, E. Łobocka, A. Strykowski and J. Bogdanski are appreciated for their help in handling with the Mineralogical Museum – University of Wrocław nephrite collection. Many thanks to A. Kumor and the owner of the Naślawice Quarry for allowing fieldwork in the quarry, and to M. Kandler for help. Thanks also to T. Larson for help with oxygen isotope analyses, and to Z. Kasztovszky, B. Maróti, and V. Szilágyi for PGAA analyses. L. Jeak is appreciated for her help with the microprobe work. Many thanks go to Katalin T. Biró, A. Szuszkiewicz, K. Turniak and J. Puziewicz for their numerous constructive suggestions. R. Kryza, D. Hovorka, and an anonymous reviewer are appreciated for their constructive reviews, which contributed much to the improvement of the manuscript. Thanks also to T. Peryt and S. Mikulski for their editorial corrections.

REFERENCES

- Adamo, I., Bocchio, R., 2013.** Nephrite jade from Val Malenco, Italy: review and update. *Gems and Gemology*, **49**: 98–106.
- Adams, C.J., Beck, R.J., Campbell, H.J., 2007.** Characterisation and origin of New Zealand nephrite jade using its strontium isotopic signature. *Lithos*, **97**: 307–322.
- Aitchison, J.C., Ireland, T.R., Blake Jr., M.C., Flood, P.G., 1992.** 530 Ma zircon age for ophiolite from the New England orogen: oldest rocks known from eastern Australia. *Geology*, **20**: 125–128.
- Barkov, A.Y., Nixon, G.T., Levson, V.M., Martin, R.F., 2009.** Patterns of zonation in magnesiochromite-chromite from placers of British Columbia, Canada. *Canadian Mineralogist*, **47**: 953–968.
- Beutell, A., Heinze, K., 1914.** Nephrit von Reichenstein in Schlesien, ein Übergangsprodukt vom Salit zum Serpentin. *Centralblatt für Mineralogie, Geologie und Paläontologie*, **15**: 553–560.
- Borkowska, M., Marie, F.A., Narbski, W., Pin, C., 1989.** General mineralogical, geochemical and petrologic characteristics of the Nowa Ruda gabbro-diabasic complex. In: *Lower and Upper Paleozoic metabasites and ophiolites of the Polish Sudetes – guidebook of excursions in Poland* (eds. W. Narbski and A. Majerowicz): 102–111. Institute of Geological Sciences, Wrocław University, Wrocław.
- Cuevas, J., Esteban, J.J., Tubía, J.M., 2006.** Tectonic implications of the granite dyke swarm in the Ronda peridotites (Betic Cordilleras, Southern Spain). *Journal of the Geological Society*, **163**: 631–640.
- Devine, F., Murphy, D.C., Carr, S.D., 2007.** Yukon-Tanana terrane in the southern Campbell Range, Finlayson Lake belt, southeastern Yukon: the geological setting of retrogressed eclogite of the Klatsa metamorphic complex. *Canadian Journal of Earth Sciences*, **44**: 317–336.
- Dietrich, V., de Quervain, F., 1968.** Die Nephrit-Talklagerstätte Scortaseo (Puschlav, Kanton Graubünden). *Übersicht der Weiteren Nephritfunde der Schweizer Alpen Insbesondere der Vorkommen im Oberhalbstein (Graubünden). Beiträge zur Geologie der Schweiz, Geotechnische Serie*, **46**.
- Dubiska, E., 1995.** Rodingites of the eastern part of the Jordanów-Gogołów serpentinite massif, Lower Silesia, Poland. *Canadian Mineralogist*, **33**: 585–608.
- Dubiska, E., Bylina, P., Kozłowski, A., Dörr, W., Nejbort, K., Schastok, J., Kulicki, C., 2004.** U-Pb dating of serpentinization: hydrothermal zircon from a metasomatic rodingite shell (Sudetic ophiolite, SW Poland). *Chemical Geology*, **203**: 183–203.
- De Hoog, J.C.M., Janák, M., Vrabec, M., Froitzheim, N., 2009.** Serpentinised peridotites from an ultrahigh-pressure terrane in the Pohorje Mts. (Eastern Alps, Slovenia): geochemical constraints on petrogenesis and tectonic setting. *Lithos*, **109**: 209–222.
- Derbyshire, E.J., O’Driscoll, B., Lenaz, D., Gertisser, R., Kronz, A., 2013.** Compositionally heterogeneous podiform chromitite in the Shetland Ophiolite Complex (Scotland): implications for chromitite petrogenesis and late-stage alteration in the upper mantle portion of a supra-subduction zone ophiolite. *Lithos*, **162–163**: 279–300.
- Esteban, J.J., Cuevas, J., Tubía, J.M., Liati, A., Seward, D., Gebauer, D., 2007.** Timing and origin of zircon-bearing chlorite schists in the Ronda peridotites (Betic Cordilleras, Southern Spain). *Lithos*, **99**: 121–135.
- Gadzicki, J., 1960.** Szczegółowa mapa geologiczna Sudetów, 1:25 000, arkusz Sobótka (in Polish). *Wyd. Geol., Warszawa*.
- Gil, G., 2011.** Mineral chemistry of the As-bearing ore minerals from Złoty Stok nephrites – preliminary results. *Mineralogia Special Papers*, **38**: 92–93.
- Gil, G., 2013.** Petrographic and microprobe study of nephrites from Lower Silesia (SW Poland). *Geological Quarterly*, **57** (3): 395–404.

- Grapes, R.H., Yun, S.T., 2010.** Geochemistry of a New Zealand nephrite weathering rind. *New Zealand Journal of Geology and Geophysics*, **53**: 413–426.
- Gunia, P., 1992.** Petrology of the ultrabasic rocks from the Braszowice-Brze nica Massif (Fore-Sudetic Block). *Geologia Sudetica*, **26**: 119–170.
- Gunia, P., 2000.** Nephrite from South-Western Poland as potential raw material of the European Neolithic artefacts. *Krystalinikum*, **26**: 167–171.
- Harlow, G.E., Sorensen, S.S., 2001.** Jade: occurrence and metasomatic origin. *The Australian Gemmologist*, **21**: 7–10.
- Harlow, G.E., Sorensen, S.S., 2005.** Jade (nephrite and jadeite) and serpentinite: metasomatic connections. *International Geology Review*, **47**: 113–146.
- Heflik, W., 1974.** Nefryt. (in Polish). *Nauka dla wszystkich*, **229**.
- Heflik, W., 2010.** About some decorative gems from the Lower Silesia and their significance in the development of material culture (in Polish with English summary). In: *Dzieje górnictwa – element europejskiego dziedzictwa kultury* (eds. P.P. Zagó d on and M. Madziarz): 139–148. Oficyna Wydawnicza Politechniki Wrocławskiej, Wrocław.
- Heflik, W., Natkaniec-Nowak, L., Duma ska-Słowik, M., 2014.** Rodingite from Nasławice and the other occurrences of these rocks in Lower Silesia (SW Poland). *Geological Quarterly*, **58** (1): 31–40.
- Jamrozik, L., 1981a.** General geology and tectonics of the serpentinite-gabbroic Braszowice-Grochowa massif. In: *Ophiolites and initialites of northern border of the Bohemian Massif* (ed. W. Narbski): 95–103. Academy of Sciences of German Democratic Republic, Central Institute for Physics of the Earth, Potsdam-Freiberg.
- Jamrozik, L., 1981b.** General geology of the Nowa Ruda serpentinite-gabbro-diabasic massif. In: *Ophiolites and initialites of northern border of the Bohemian Massif* (ed. W. Narbski): 120–128. Academy of Sciences of German Democratic Republic, Central Institute for Physics of the Earth, Potsdam-Freiberg.
- J drysek, M.O., Hałas, S., 1990.** The origin of magnesite deposits from the Polish Foresudetic Block ophiolites: Preliminary $\delta^{13}\text{C}$ and $\delta^{18}\text{O}$ investigations. *Terra Nova*, **2**: 154–159.
- J drysek, M.O., Jasi ska, B., Boduch, M., 1991.** Serpentinization of ultramafic rocks of the Gogołów-Jordanów Serpentine Massif (SW Poland) in the light of isotope studies of hydrogen and oxygen. *Mineralogia Polonica*, **22**: 61–76.
- Kostov, R.I., Prochirov, C., Stoyanov, C., Csedreki, L., Simon, A., Szikszai, Z., Uzonyi, I., Gaydarska, B., Chapman, J., 2012.** Micro-PIXE geochemical fingerprinting of nephrite Neolithic artifacts from Southwest Bulgaria. *Geoarchaeology: an International Journal*, **27**: 457–469.
- Kryza, R., 2011.** Early Carboniferous (~337 Ma) granite intrusion in Devonian (~400 Ma) ophiolite of the Central-European Variscides. *Geological Quarterly*, **55** (3): 213–222.
- Kryza, R., Pin, C., 2010.** The Central-Sudetic ophiolites (SW Poland): petrogenetic issues, geochronology and palaeotectonic implications. *Gondwana Research*, **17**: 292–305.
- Kuroda, J., Ohkouchi, N., Ishii, T., Tokuyama, H., Taira, A., 2005.** Lamina-scale analysis of sedimentary components in Cretaceous black shales by chemical compositional mapping: implications for paleoenvironmental changes during the Oceanic Anoxic Events. *Geochimica et Cosmochimica Acta*, **69**: 1479–1494.
- Leake, B.E., Woolley, A.R., Arps, C.E.S., Birch, W.D., Gilbert, C.M., Grice, J.D., Hawthorne, F.C., Kato, A., Kisch, H.J., Krivovichev, V.G., Linthout, K., Laird, J., Mandarino, J.A., Maresch, W.V., Nickel, E.H., Rock, N.M.S., Schumacher, J.C., Smith, D.C., Stephenson, N.C.N., Ungaretti, L., Whittaker, E.J.W., Youzhi, G., 1997.** Nomenclature of amphiboles: report of the subcommittee on amphiboles of the international mineralogical association, commission on new minerals and mineral names. *Canadian Mineralogist*, **35**: 219–246.
- Ling, X., Schmädicke, E., Wu, R., Wang, S., Gose, J., 2013.** Composition and distinction of white nephrite from Asian deposits. *Neues Jahrbuch für Mineralogie-Abhandlungen (Journal of Mineralogy and Geochemistry)*, **190/1**: 49–65.
- Liu, Y., Deng, J., Shi, G., Lu, T., He, H., Ng, Y.-N., Shen, C., Yang, L., Wang, Q., 2010.** Chemical zone of nephrite in Alamas, Xinjiang, China. *Resource Geology*, **60**: 249–259.
- Liu, Y., Deng, J., Shi, G., Sun, X., Yang, L., 2011a.** Geochemistry and petrogenesis of placer nephrite from Hetian, Xinjiang, Northwest China. *Ore Geology Reviews*, **41**: 122–132.
- Liu, Y., Deng, J., Shi, G., Yui, T.-F., Zhang, G., Abuduwayiti, M., Yang, L., Sun, X., 2011b.** Geochemistry and petrology of nephrite from Alamas, Xinjiang, NW China. *Journal of Asian Earth Sciences*, **42**: 440–451.
- Łapot, W., 2004.** Peculiar nephrite from the East Saian Mts (Siberia). *Mineralogia Polonica*, **35**: 49–58.
- Łobos, K., Sachanbi ski, M., Pawlik, T., 2008.** Nephrite from Nasławice in Lower Silesia (SW Poland) (in Polish with English summary). *Przeł d Geologiczny*, **56**: 991–999.
- Maciejewski, S., 1966.** Nephrite rocks of the Sobótka Massif (in Polish with English summary). In: *Z Geologii Ziemi Zachodnich, Sesja Naukowa Dwudziestolecia Polskich Bada 1945–1965* (ed. J. Oberc): 459–468. Towarzystwo Rozwoju Ziemi Zachodnich, Wrocław.
- Majerowicz, A., 1963.** The granite of the environs of Sobótka and its relation to country rocks (in Polish with English summary). *Archiwum Mineralogiczne*, **24**: 127–238.
- Majerowicz, A., 1979.** Wyst powanie rodingitów w masywie serpentynitowym Gogołów-Jordanów (in Polish). *Przeł d Geologiczny*, **27**: 43–44.
- Majerowicz, A., 1984.** Petrography and genesis of rodingites in serpentinites of the l a ophiolitic group (in Polish with English summary). *Geologia Sudetica*, **18**: 109–132.
- Majerowicz, A., 2006.** Krótki przewodnik terenowy po skałach ofiolitowego zespołu l y oraz ich petrologicznej i geologicznej historii (in Polish). Wrocław University Press, Wrocław.
- Makepeace, K., Simandl, G.J., 2001.** Jade (nephrite) in British Columbia, Canada. Program and Extended Abstracts for 37th Forum on the Geology of Industrial Minerals, **37** (2001): 209–210.
- Mazur, S., Aleksandrowski, P., Kryza, R., Oberc-Dziedzic, T., 2006.** The Variscan orogen in Poland. *Geological Quarterly*, **50** (1): 89–118.
- Middleton, A., 2006.** JADE – Geology and Mineralogy. In: *Gems* (ed. M. O'Donoghue): 332–354. Elsevier Ltd., Oxford.
- Mierzejewski, M.P., Abdel-Wahed, M., 2000.** Overlapping thrust faults within the Gogołów-Jordanów serpentinite massif (SW Poland): evidence for the obduction of l a ophiolite complex. In: *Tectonics of the l a Ophiolite and its Influence on the Distribution of Some Mineral Ores and Ground Water* (ed. M.P. Mierzejewski): 29–41. Institute of Geological Sciences, Wrocław University, Wrocław.
- Morimoto, N., Fabries, J., Ferguson, A.K., Ginzburg, I.V., Ross, M., Seifert, F.A., Zussman, J., Aoki, K., Gottardi, G., 1988.** Nomenclature of pyroxenes. *American Mineralogist*, **73**: 1123–1133.
- Narbski, W., Wajsprych, B., Bakun-Czubarow, N., 1982.** On the nature, origin and geotectonic significance of ophiolites and related rock suites in the Polish part of the Sudetes. *Ofioliti*, **7**: 407–428.
- Péterdi, B., Szakmány, G., Judik, K., Dobosi, G., Kasztovszky, Z., Szilágyi, V., Maróti, B., Bend, Z., Gil, G., 2014.** Petrographic and geochemical investigation of a stone adze made of nephrite from the Balaton szöd – Temeti d l site (Hungary), with a review of the nephrite occurrences in Europe (especially in Switzerland and in the Bohemian Massif). *Geological Quarterly*, **58** (1): 181–192.
- Oliver, G.J.H., Corfu, F., Krogh, T.E., 1993.** U-Pb ages from SW Poland: Evidence for a Caledonian suture zone between Baltica and Gondwana. *Journal of the Geological Society*, **150**: 355–369.
- Proenza, J.A., Ortega-Gutiérrez, F., Camprubí, A., Tritlla, J., Elías-Herrera, M., Reyes-Salas, M., 2004.** Paleozoic serpentinite-enclosed chromitites from Tehuizingo (Acatlán Complex,

- southern Mexico): a petrological and mineralogical study. *Journal of South American Earth Sciences*, **16**: 649–666.
- Sachs, A., 1902.** Der "Weissstein" des Jordansmühler Nephritvorkommens. *Centralblatt für Mineralogie, Geologie und Paläontologie*, **1902**: 385–396.
- Schulze, D.J., 2003.** A classification scheme for mantle-derived garnets in kimberlite: a tool for investigating the mantle and exploring for diamonds. *Lithos*, **71**: 195–213.
- Sharp, Z.D., 1990.** A laser-based microanalytical method for the in situ determination of oxygen isotope ratios of silicates and oxides. *Geochimica et Cosmochimica Acta*, **54**: 1353–1357.
- Sherer, R.L., 1972.** Geology of the Sage Creek nephrite deposit, Wyoming. *Contributions to Geology*, **11**: 83–86.
- Simandl, G.J., Riveros, C.P., Schiarizza, P., 2000.** Nephrite (jade) deposits, Mount Ogden area, Central British Columbia (NTS 093N 13W). *Geological Fieldwork*, **1999**: 339–347.
- Sinkankas, J., 1959.** Jade. In: *Gemstones of North America* (ed. J. Sinkankas): 236–259. D. Van Nostrand Company Inc., Princeton.
- Siqin, B., Qian, R., Zhuo, S., Gan, F., Dong, M., Hua, Y., 2012.** Glow discharge mass spectrometry studies on nephrite minerals formed by different metallogenic mechanisms and geological environments. *International Journal of Mass Spectrometry*, **309**: 206–211.
- Traube, H., 1885a.** Ueber den Nephrit von Jordansmühl in Schlesien. *Neues Jahrbuch für Mineralogie, Geologie und Palaeontologie* (Beilage-Band), **3**: 412–427.
- Traube, H., 1885b.** Über den Nephrit von Jordansmühl in Schlesien. *Neues Jahrbuch für Mineralogie, Geologie und Palaeontologie*, **2**: 91–94.
- Traube, H., 1887.** Ueber einen neuen Fund von anstehendem Nephrit bei Reichenstein in Schlesien. *Neues Jahrbuch für Mineralogie, Geologie und Palaeontologie*, **2**: 275–278.
- Traube, H., 1888.** Nephrit. In: *Die Minerale Schlesiens* (ed. H. Traube): 148. J.U. Kern's Verlag, Breslau.
- Trepka, S., Mierzejewski, M., 1961.** Szczegółowa mapa geologiczna Sudetów, 1:25 000, arkusz Jordanów I ski (in Polish). *Wyd. Geol., Warszawa*.
- Turniak, K., Mazur, S., Domańska-Siuda, J., Szuskiewicz, A., 2014.** SHRIMP U-Pb zircon dating for granitoids from the Strzegom-Sobótka Massif, SW Poland: constraints on the initial time of Permo-Mesozoic lithosphere thinning beneath Central Europe. *Lithos*, **208–209**: 415–429.
- Valley, J.W., Kitchen, N., Kohn, M.J., Neindorf, C.R., Spicuzza, M.J., 1995.** UWG-2, a garnet standard for oxygen isotope ratios: Strategies for high precision and accuracy with laser heating. *Geochimica et Cosmochimica Acta*, **59**: 5223–5231.
- Wan, H.-M., Yeh, C.-L., 1984.** Uvarovite and grossular from the Fengtien nephrite deposits, eastern Taiwan. *Mineralogical Magazine*, **48**: 31–37.
- Yui, T.-F., Kwon, S.-T., 2002.** Origin of a dolomite-related jade deposit at Chuncheon, Korea. *Economic Geology*, **97**: 593–601.
- Yui, T.-F., Yeh, H.-W., Wang Lee, C., 1988.** Stable isotope studies of nephrite deposits from Fengtien, Taiwan. *Geochimica et Cosmochimica Acta*, **52**: 593–602.